Bedrijfstakonderzoek
BTO 2021.052 | September 2021

De invloed van de drinkwater-samenstelling op uitloging van cementhoudende leidingmaterialen: een model

Joint Research Programme

KWR

Bridging Science to Practice

Report

De invloed van de drinkwatersamenstelling op uitloging van cementhoudende leidingmaterialen: een model

A model for the influence of drinking water composition on leaching of cement-based pipes

BTO 2021.052 | September 2021

Dit onderzoek is onderdeel van het collectieve Bedrijfstakonderzoek van KWR, de waterbedrijven en Vewin.

Project number
402045-211

Project manager
Nellie Slaats

Client
BTO - Bedrijfsonderzoek

Author(s)
Alex Hockin MSc, Martin Korevaar PhD, Karel van Laarhoven PhD

Quality Assurance
Mirjam Blokker PhD

Sent to
This report is distributed to BTO-participants and is public.

Keywords

asbestos cement, leaching, PHREEQC, drinking water composition, saturation index

Year of publishing
2021

More information
Alex Hockin
T 06-15608101
E alex.hockin@kwrwater.nl

PO Box 1072
3430 BB Nieuwegein
The Netherlands

T +31 (0)30 60 69 511
F +31 (0)30 60 61 165
E info@kwrwater.nl
I www.kwrwater.nl

Samenvatting

In cementhoudende drinkwaterleidingen is een belangrijke wettelijke eis voor de chemische samenstelling van drinkwater dat de verzadigingsindex (SI) van calciet hoger is dan -0,2. Deze parameter is opgenomen om de uitloging van asbestcement en andere cementhoudende leidingen te beperken. Uitloging van cementhoudende leidingen leidt tot verzwakking, wat kan resulteren in leidingbreuken. Een typische aanpak om dit te verhelpen is drinkwater te produceren dat voldoende verzadigd is met calciumcarbonaat, waardoor op de binnenwanden van de leidingen een laag calciumcarbonaatneerslag ontstaat die de uitloging uit de wand blokkeert en bescherming biedt tegen aantasting. De effectiviteit van de SI als maatgevende indicator is echter niet eenduidig, omdat de vorming van de beschermende laag complex is, afhankelijk is van de volledige drinkwatersamenstelling en niet alle lagen evenveel bescherming bieden tegen uitloging.

In dit project is de chemische degradatie van asbestcement drinkwaterleidingen gesimuleerd met een chemische speciatiesoftware (PHREEQC) via de python programmeertaal (PhreeqPython). Het toegepaste model bestaat uit twee stappen. In de eerst stap wordt het chemisch evenwicht tussen buiswand en water bepaald, terwijl in de tweede stap de diffusie door de buiswand wordt gemodelleerd. De correcte toepassing van het evenwichtsmodel werd onafhankelijk van het diffusiemodel geverifieerd door het resultaat ervan te vergelijken met literatuurwaarden voor verschillende initiële watersamenstellingen. Het diffusiemodel combineert het chemisch evenwichtsmodel met terugkoppeling van de chemische afbraak naar de bijbehorende fysische veranderingen in het cement (bv. porositeit) om het uitloogproces kwantitatief te voorspellen voor een gegeven watersamenstelling. Het diffusiemodel werd gevalideerd met experimenten uit de literatuur voor twee watersamenstellingen en verschillende water-cement verhoudingen. Uit de eerst resultaten blijkt dat het model gevoelig is voor de initiële water/cementverhouding en daarom is een meer gedetailleerde gevoeligheidsanalyse noodzakelijk en reeds gepland voor een vervolgproject. De resultaten waren echter voldoende om met het model een eerste indicatie te kunnen geven van de effecten van verschillende watersamenstellingen op uitloging.

In overleg met de projectgroep werden vier drinkwatersamenstellingen gekozen on door te rekenen met het model: de vier locaties waren Lekkerkerk (Oasen), Nijverdal (Vitens), Andijk (PWN) en Hoogeveen (WMD). De samenstellingen werden zo gekozen dat er een spreiding in de drinkwatersamenstelling was en dat er locaties bij waren die regelmatig (Nijverdal, Andijk) en soms (Lekkerkerk) problemen hadden met het voldoen aan de SI-criteria, en een locatie waar geen problemen waren (Hoogeveen). Eerst werd het chemische model gebruikt, dat de mineralogische veranderingen in cement simuleert wanneer het wordt blootgesteld aan opeenvolgende poriënvolumes water (geen terugkoppeling van verlies van mineralen naar de porositeit). Voor alle gevallen laten de resultaten duidelijk zien dat tijdens het uitlogen de verschillende mineralen in het cement in dezelfde volgorde oplossen; alleen de snelheid waarmee dit gebeurt verschilt. Zoals verwacht voorspelden de grootte en het teken van de SI het precipitatie/oplossingsgedrag van calciet te stoppen. Zoals verwacht was er bij een negatieve SI sprake van ontbinding van calciet in de laatste fase van de cementafbraak, terwijl een hogere, positievere SI overeenkwam met de hoogste neerslagsnelheid van calciet.

Vervolgens werd het diffusiemodel toegepast voor een simulatie van 7 jaar en er werden aanzienlijke verschillen tussen de resultaten van de watersamenstellingen waargenomen. Interessant is dat het model, in tegenstelling tot het chemisch model, een eerste indicatie geeft dat SI alleen niet voldoende is om de uitlogingssnelheid en de chemische evolutie van cementbuizen te voorspellen en dat er een complex verband bestaat tussen cementuitloging en watersamenstelling. In het model resulteerde de neerslag van calciet in een verminderde porositeit, die op haar beurt de diffusie in de rest van de buiswand verminderde en zo de totale uitloging verminderde, hetgeen een eerste aanwijzing geeft voor een mogelijke beschermlaag. In een vervolgproject zal de

relatie tussen uitlooggedrag en andere indexparameters, bijvoorbeeld Calcium Carbonaat Neerslag Potentieel (CCPP), agressief CO2, worden onderzocht in een systematische gevoeligheidsstudie. Bovendien zal meer kennis worden vergaard over de poreuze aard van calcietlagen op pijpwanden. Tenslotte moet het model verder gevalideerd worden met case studies uit de praktijk.

Contents

1 Introductie

Achtergrond en belang

Er worden veel verschillende eisen die gestelld aan de chemische samenstelling van het drinkwater (Slaats et al., 2013). Een van de eisen is dat de verzadigingsindex van calciet, vaak SI genoemd, boven de waarde van -0,2 ligt (Drinkwaterbesluit, Bijlage A in Tabel IIIa, Indicatoren –Bedrijfstechnische parameters). Sommige waterbedrijven moeten op dit moment chemicaliën doseren om de SI op het wettelijke niveau te krijgen. Zowel vanuit financieel als duurzaamheidsoogpunt wordt deze dosering het liefs tot een minimum beperkt.

De SI is opgenomen om de uitloging van asbestcement en cementhoudende leidingen te beperken: in voldoende verzadigd water kan een deklaagje van calciumcarbonaat bestaan op de binnenwand van leidingen (LeRoy et al., 1996; Schock et al., 1981). Een dergelijk deklaagje kan vervolgens als bescherming dienen tegen de degradatie van cementhoudende leidingen via uitloging van calciumhydroxide. Het is belangrijk om uitloging te voorkomen omdat dit leidt tot verzwakking van de buis.

De effectiviteit van de SI als maatgevende indicator voor uitloging onduidelijk is (o.a. Kuai et al., 2015; Le et al., 2016; Rossum et al., 1983; Torres et al., 2015; WHO, 2011). Ten eerste is het vormen van de deklaagjes een complex proces dat afhangt van de complete drinkwatersamenstelling, niet alleen van de aanwezige calcium- en waterstofcarbonaatconcentratie. Ten tweede is uit experimenten gebleken dat deklaagjes niet in alle gevallen evenveel bescherming bieden tegen de uitloging van calciumhydroxide (Shock en Buelow, 1981).

Het doel van dit project, en volgende fasen, is om meer inzicht te krijgen in de invloed van de drinkwatersamenstelling op de cement uitloging als tijdsafhankelijk proces. Hiervoor wordt het proces gesimuleerd met chemische speciatiesoftware (e.g. PHREEQC). Op basis van inzicht in deze aspecten kunnen drinkwaterbedrijven de drinkwatersamenstelling beïnvloeden zodanig dat de uitloging van hun cementhoudende leidingen goed is te beheersen. Dit zal leiden tot een toekomstbestendiger leidingnet. De gemodelleerde koppeling tussen drinkwatersamenstelling en uitloging kan een essentiële bijdrage leveren aan een heroverweging van (van de drinkwatersamenstelling afgeleide) indexparameters zoals SI, TACC (totaal afzetbaar calcium carbonaat) of CCPP (calcium carbonate precipitation potential) als maat voor het risico op uitloging. De inzichten in dit project kunnen daarmee handvatten bieden aan waterbedrijven om in gesprek te gaan over een eventuele aanpassing van de norm in het Drinkwaterbesluit.

Leeswijzer

Hoofdstuk 2 beschrijft de relevante theorie en aanpak voor cementmodellering, de implementatie van het model in PHREEQC en de verificatie van het model. Verificatie van een model controleert of het operationele model en het computationele model logisch consistent zijn, en of zij semantisch consistent zijn met het conceptuele model dat in de conceptualisatiestap werd ontwikkeld.

Hoofdstuk 3 presenteert de validatie van het model aan de hand van experimenten met uitloging uit de literatuur. Validatie van een model betekent dat wordt nagegaan of de met het rekenmodel verkregen resultaten inderdaad een goed (voldoende) antwoord geven op de onderzoeksvraag.

Hoofdstuk 4 beschrijft de toepassing van het model voor asbestcement en vier verschillende drinkwatersamenstellingen van de waterbedrijven.

Hoofdstuk 5 bespreekt de resultaten in de context van de Nederlandse drinkwaterwaterbedrijven, de conclusies van dit project en de aanbevelingen voor verdere modelverbetering en implementatie.

De hoofdstukken 1 en 5 zijn in het Nederlands geschreven en de hoofdstukken 2, 3 en 4 in het Engels..

2 Model Approach

2.1 Introduction

Cement is widely used in many applications, including in drinking water production and distribution. Under many conditions, cement is a durable long-lasting material. However, cement can also degrade when in contact with water for long periods, as a result of diffusion of cement components from the solid phase to the water phase. This process is known as leaching. In the long-term, leaching can result in substantial deterioration of cement-containing structures, such that failure occurs.

Leaching can be described by three processes, (1) the dissolution of the mineral of interest from the solid phase to the water phase, (2) the diffusion of the dissolved mineral in the inner to outer pores and (3) the transfer of the dissolved mineral out of the system (Richardson et al., 2002). In the case of cement leaching, the first step is the dissolution of cement minerals from the cement paste to the pore water (Figure 1 - 2), followed by the diffusion of the dissolved cement mineral from the inner pore water to the outer edge of the cement paste (in our case the inner pipe wall), which is in contact with the drinking water (Figure 1 - 3). Once the dissolved mineral has reached the inner pipe wall it is removed from the system by the diffusion into the passing drinking water (Figure 1 - 4).

In order to accurately model leaching in cement, a model will roughly consist of the following four aspects:

- The chemical composition of cement – the part of the model which specifies which elements and minerals are present;
- The thermodynamic stability of cement minerals - the part of the model governing changes in the composition of the cement through dissolution;
- Diffusive transport - the part of the model governing transport of dissolved cement components through the porous cement matrix;
- The microstructure of - gradually dissolving - cement - the part of the model that describes how changes in composition due to dissolution result in changes in transport of solutes through the porous matrix.

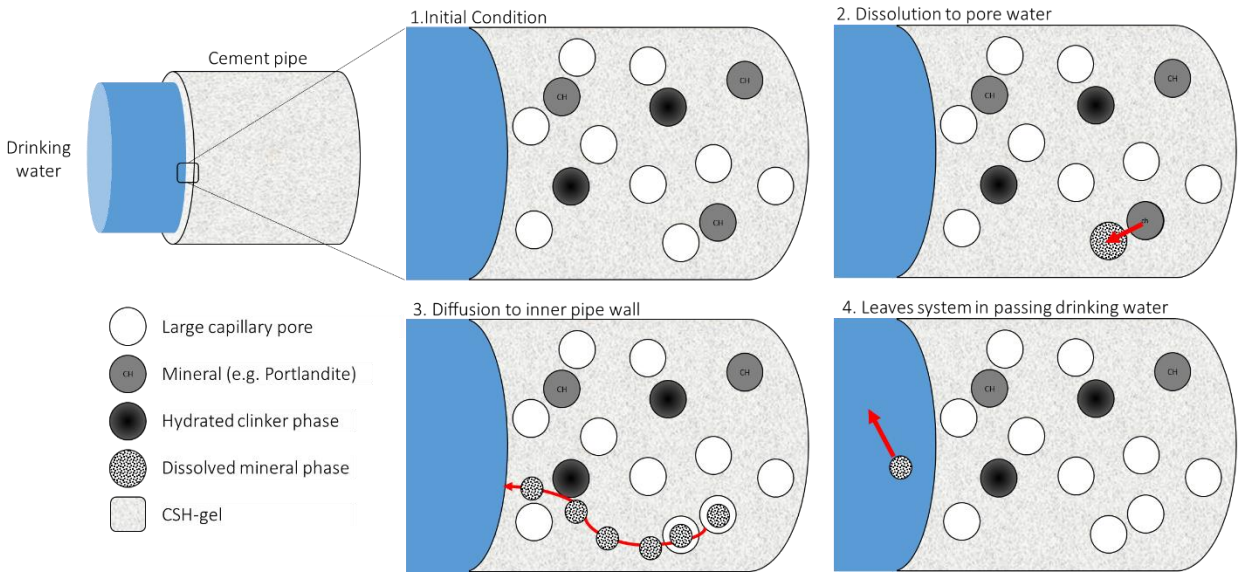

Figure 1 Schematisation of the process of cement leaching for a cement drinking water pipe. Initially, (1) cement is in contact with drinking water at the left boundary. Cement minerals and hydrated phases are present in the cement paste. (2) Dissolution of a cement mineral occurs in the pore water present in a capillary pores. (3) The dissolved mineral diffuses from the inner cement paste to the inner pipe wall. (4) The

dissolved mineral is removed from the cement by diffusion in the passing drinking water [1]CSH-gel consist of the CSH minerals (in our model the jennite- and tobermorite-like minerals) and is the primary component of Portland cement.

2.2 Theory

2.2.1 Chemical Cement Composition

Ordinary Portland Cement (OPC) consists of four major clinker phases: alite (C_3S), belite(C_2S), aluminate (C_3A) and ferrite (C_4AF) (Lothenbach et al., 2008). Clinker is the industry term for a mixture of clay and limestone which is heated at high temperature. Different types of OPC exists, the one used here is CEM I 42.5 (Table I). When cement is reacted with water, the clinker phases slowly hydrate to form cement hydrates. The cement hydrates included in are briefly described in Table 2, coming from in the thermodynamic cement database (CEMDATA07), developed by Lothenbach et al., (2008, 2006); Matschei et al., (2007). The chemical composition of cement determines the initial pore water composition and cement is rarely in thermodynamic equilibrium with the surrounding pore water. This results in the dissolution and/or precipitation of minerals in the cement-water system, which can be modelled using chemical thermodynamic models.

Table I OPC Composition (Lothenbach et al., 2008).

MINERAL	G/100 G OPC	MOL / 100 G OPC	MOLAR MASS (G/MOL)	MOL/350G OPC
CaO	62.4	1.113	56.1	3.89
SiO_2	18.9	0.315	60.1	1.10
Al_2O_3	4.4	0.043	102.0	0.15
Fe_2O_3	2.5	0.016	159.7	0.05
CaO (free)	0.6	0.011	56.1	0.04
MgO	1.4	0.035	40.3	0.12
K_2O	0.95	0.010	94.2	0.04
Na_2O	0.10	0.002	62.0	0.01
CO_2	2.1	0.048	44.0	0.17
SO_3	3.0	0.038	80.1	0.13

2.2.2 Thermodynamic stability

The dissolution or precipitation of minerals in cement is determined by the mineral thermodynamics and minerals precipitate or dissolve to achieve chemical equilibrium in the system. When a system is in equilibrium, the Gibbs free energy of the system is at a minimum and all chemical reactions are in equilibrium. Mass action equations relate changes in the Gibbs free energy of reaction the mass action constants (Jacques, 2009). In chemical equilibrium modelling, the mass action equations and conservation of mass is used to calculate the equilibrium state of a system (Appelo et al., 2005). In order to calculate the chemical equilibrium of a system, chemical modelling software are used (Parkhurst et al., 2013). PHREEQC is one such software and used in this model contains standard databases of the aqueous speciation and activity coefficients[1] of common elements.

A specialized cement thermodynamic database (CEMDATA07) has been compiled by Lothenbach et al., (2008, 2006); Matschei et al., (2007), containing mass action constants from literature and practice for cement minerals for the Gibbs Energy Minimization software (GEMS). The conversion of the GEMS database to be suitable for use in PHREEQC and calculations at temperatures other than 25 °C is described in Jacques, (2009).

[1] Activity coefficient are factors used in thermodynamics to account for deviations from ideal behaviour in a mixture of chemical substances

Table 2 Mineral phases in model and description

MINERAL	DESCRIPTION
CALCIUM-SILICATE-HYDRATES (CSH)	CSH form the main components of hydrated OPC (Jacques, 2009). In the model, the CSH phase is described by an ideal solid solution[1] of jennite ($Ca_9Si_6O_{18}(OH)_6{\cdot}8H_2O$) and tobermorite-II ($Ca_5Si_6O_{16}(OH)_2{\cdot}4H_2O$) and a pure phase of amorpheous silciumdioxide (SiO_2).
AFT-PHASES	Alumina, ferric oxide, tri-sulfate (Aft)-phases are a group of calcium sulfoaluminate hydrates, with the general formula $Ca_3(Al,Fe)(OH)_6{\cdot}12\ H_2O]_2{\cdot}X_3{\cdot}xH_2O$ where X is a doubly charged anion. Ettringite is the most important Aft-phase. Ettringite and tricarboaluminate can form a non-ideal solid solution[1], with non-dimensional Guggenheim parameters[2] a_o= -0.823, a_1 =2.82.
AFM-PHASES	Alumina, ferric oxide, mono-sulfate (Afm)-phases are a complex group of calcium aluminate hydrates, with the general formula $[Ca_2(Al,Fe)(OH)_6)]{\cdot}X{\cdot}xH_2O$ where X is a single charged anion. Afm-phases include C_2AH_8, C_4AH_{13}, monosulfoaluminate, monocarboaluminate, hemicarboaluminate, stratlingite, amorphous $Al(OH)_3$ and CAH_{10}. A non-ideal solid solution of hydroxyl-AFm (C_4AH_{13}) and monosulfoaluminate with non-dimensional Guggenheim parameters a_o= 0.188, a_1 =2.849.
HYDROGARNET	The main hydrogarnate (Ca3Al2(OH)12) phases is included (hydrogarnetOH). The siliceous and iron hydrogarnet forms are not included in the model (siliceous hydrogarnet is not present in calcite systems (Jacques et al., 2009) and iron phases were not included in the model).
HYDROTALCITE	Two forms of hydrotalcite are included; (Mg4Al2(OH)14:3H2O) and a carbonate form (Mg4Al2(OH)12CO3:3H2O).
HYPOTHETICAL PHASES	Two hypothetical phases were added to in the CEMDATA07 database: Na_2O (log k = 24.94) and K_2O (log k = 25.71). These phases were added to control the concentration of sodium and potassium during the initial phases of cement degradation.
OTHER PHASES	Other cement minerals included: calcite, portlandite, gypsum, anhydrite, brucite and gibbsite. Iron was not included in the model as (Jacques et al., 2009) found it led to unnecessarily complicated calculations and its inclusion had no effect on the evolution of pH, element concentrations and solid phase composition. Therefore we assume that iron also does not affect the results of our simulations. The validity and consequences of this assumption are discussed in chapter 5 and will be explored further in a follow-up project.

[1]in an ideal solid solution, the activity coefficient of the mixture is equal to 1 while in non-ideal solid solutions, the activity coefficients are great or less than 1.

[2]the excess free-energy of mixing for non-ideal solid solutions can be modelled with the guggenheim series expansion, of which the first two terms are the non-dimensional guggenheim parameters (Appelo et al., 2005).

2.2.3 Diffusive transport

Diffusion is the resulting movement of particles from regions of higher to lower concentration, as described by Fick's Law (Appelo et al., 2005);

$$F = -D\,\frac{\partial c}{\partial x} \qquad \textit{Eq. 1}$$

Where F is the flux (mol/s/m^2), D is the diffusion coefficient (m^2/s) and is the concentration (mol/m^3).

The diffusion coefficient depends on, among other things, the ion size, the temperature and interaction with other diffusing species due to species charge. Oppositely charge species can accelerate while similarly charged species can retard diffusion (Appelo et al., 2005). Detailed data on the diffusion coefficients for elements is not always available, therefore for multi-component diffusion an average diffusion coefficient ($1.3*10^{-9}$ m^2/s at 25 °) in free water is commonly used (Appelo et al., 2005);

Diffusion of elements in porous systems must travel longer distances than in 'free' water. To account for this additional travel distance, the effective diffusion coefficient (D_e) is defined;

$$D_e = D\ \varepsilon_w \qquad \textit{Eq. 2}$$

Where ε_w is the water-filled porosity [-]. In saturated systems, ε_w is equal to the porosity. PHREEQC's solves the advection-dispersion equation (Appelo et al., 2005);

$$\frac{\partial C_j}{\partial t} = -v\frac{\partial C_j}{\partial x} - \frac{\partial q}{\partial t} + D_L\frac{\partial^2 C_j}{\partial x^2} \qquad \textit{Eq. 3}$$

where *C* is concentration in moles per kilogram water (kgw) [mol/kgw], *t* is time [s], *v* is porewater flow velocity [m/s], *x* is distance [m], D_L is the hydrodynamic dispersion coefficient [m^2/s], *q* is concentration in the solid phase (expressed as mol/kgw in the pores). In cement systems, the advection of water through the cement paste is assumed to be negligible and therefore only diffusive transport was modelled in PHREEQC. In PHREEQC, the diffusive transport depends on the diffusion coefficient for the element of interest and the porosity of the porous media. During cement leaching, the loss of cement minerals results in changing porosity over time. Therefore the cement microstructure must also be taken into account in the model.

2.2.4 Cement microstructure

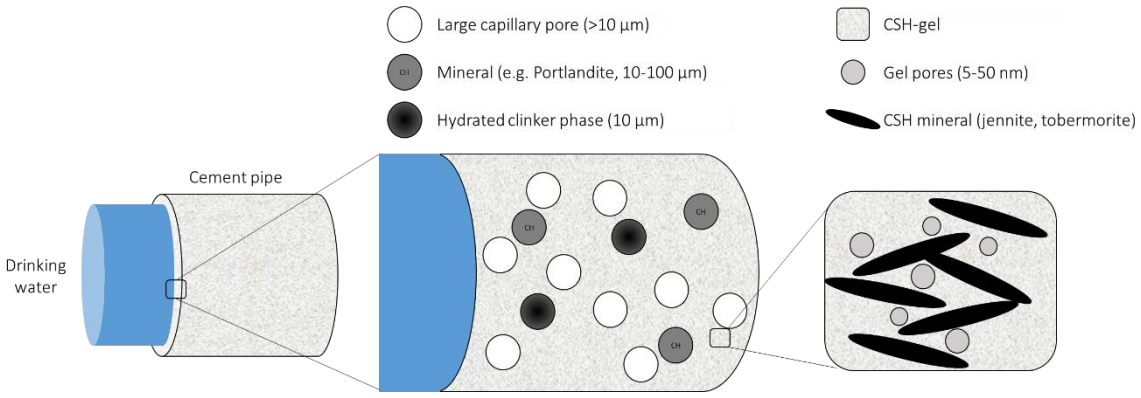

Figure 2 Conceptual model of the phases and porosity of cement. Cement consists of hydrated clinker, minerals, CSH-gel and capillary pores. Within the CSH-gel there are the CSH minerals (in our model jennite and tobermorite) and gel pores. Adapted from (Lemarchand, 2009)

Cement is a complex, multi-scale porous media (see Figure 2 Conceptual model of the phases and porosity of cement. Cement consists of hydrated clinker, minerals, CSH-gel and capillary pores. Within the CSH-gel there are the CSH minerals (in our model jennite and tobermorite) and gel pores. Adapted from (Lemarchand, 2009)Figure 2). We use the well-established cement model of Powers et al., (1946) as reviewed by Brouwers, (2004) to describe the volume fractions of the cement which are applied to estimate the porosity of the cement at different scales. The cement consists of minerals (e.g. portlandite, calcite etc.), capillary pores (0.1-1 µm) and a CSH-gel. The CSH-gel itself contains small gel pores (5-50 nm) and CSH-minerals. The CSH minerals in our model are the jennite- and tobermorite-like minerals. The cement model for our purposes can be simplified to three volume fractions, the

hydrated cement (hc) fraction, consisting of the different cement minerals; the gel pores fraction; and the capillary pores fraction (Figure 3). Together, the hydrated cement and the gel porosity form the hydration product (hp).

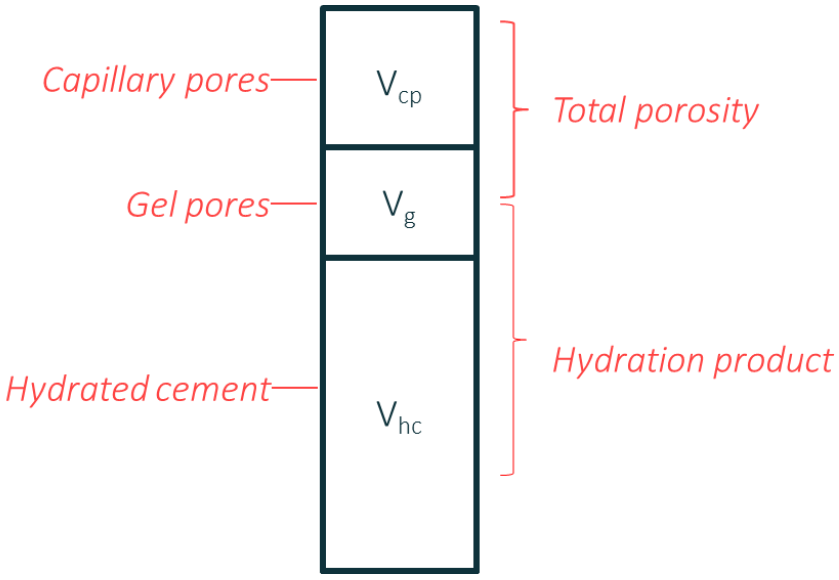

Figure 3 Simplified cement model of the volume of hydrated cement (bc), the gel pores (g) and capillary pores (cp), as based on the model of (Powers et al., 1946)

In cement-aggregate systems, such as concrete, there is an additional phase known as the interfacial transition zone (ITZ). The ITZ is a zone between the bulk cement paste and aggregate particles like pebbles or asbestos fibers(Oh et al., 2004). This zone is important in composite systems, because it substantially facilitates transport. In the case of asbestos cement, however, the importance of the ITZ is negligible because the asbestos fibers are not thick enough to influence the porosity of the surrounding cement (Bentur et al., 1999). The ITZ is therefore not considered in this study.

To describe the changes in porosity during leaching, the gel and capillary porosity should be defined. The gel porosity is a function of the volume of CSH-gel, while the capillary porosity is a function of the water to cement (w/c) ratio and the degree of hydration of the cement (α) (Patel et al., 2018). In fully hydrated cement (α= 1) all cement clinker has reacted and no unreacted cement is left. In practice, the degree of hydration is less than 1 and can be calculated from empirical formulas from literature (Bejaoui et al., 2007). Similarly, the relationship between the capillary porosity and the w/c ratio has also been empirically related. With increasing w/c ratios, the initial capillary porosity of cement increases. This is because there is a minimum w/c ratio needed to hydrate the clinker, and water added in excess of the minimum results in additional capillary pores (Brouwers, 2004).

The main transport path through cement is through the capillary pores. However, the gel pores also contribute and play an important role at very low capillary porosity (Oh et al., 2004). The critical capillary porosity (ϕ_{ccp}) is the percolation threshold, below which there is no transport through the capillary pores (Figure 4). In cement, unlike other solid media, the CSH-gel (in our case the jennite- and tobermorite-like minerals) also contain small, gel pores and there is transport through the gel pores below the critical capillary porosity (Oh et al., 2004).

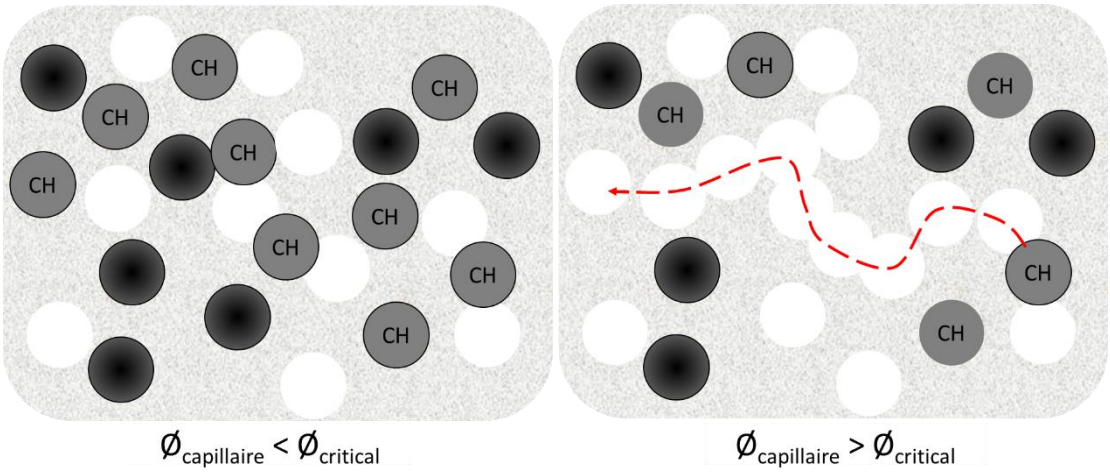

Figure 4 Visualization of the connectivity of the capillary pores (open circles). Grey and black cicles represent the cement minerals and the light grey background represents the CSH-gel. Left: below the critical capillary porosity, capillary pores are disconnected and diffusion (red line) through capillary pores does not occur. Right: above the critical capillary porosity, capillarry pores are connected and diffusion through capillary pores occurs.

As a result of the percolation threshold, it is difficult to model the diffusion through cement when the capillary porosity approaches the critical capillary porosity. To overcome this limit, we use the general effective medium (GEM) equation (Oh et al., 2004), which allows the calculation of the diffusion through cement near the critical capillary porosity (Figure 5, Eq. 4 & Eq. 5). The GEM equation allows for the calculation of non-zero solid-phase conductivity as a result of diffusion through the gel pores and gives the effective diffusivity of the porous media (D_p/D_0);

$$\frac{D_p}{D_0} = \left[\mathrm{m}_{\emptyset} + \sqrt{m_{\emptyset}^2 + \frac{\emptyset_{ccp}}{1-\emptyset_{ccp}} \left(\frac{D_s}{D_0}\right)^{\frac{1}{n}}} \right]^n \qquad \textit{Eq. 4}$$

$$\mathrm{m}_{\emptyset} = \frac{1}{2}\left[\left(\frac{D_s}{D_0}\right)^{\frac{1}{n}} + \frac{\emptyset_{ccp}}{1-\emptyset_c}\left(1 - \left(\frac{D_s}{D_0}\right)^{\frac{1}{n}}\right) - \frac{\emptyset_{ccp}}{1-\emptyset_{ccp}} \right] \qquad \textit{Eq. 5}$$

Where $\frac{D_S}{D_0}$ is normalized diffusivity of the solid phase (when the capillary porosity is zero), n is the Archie's constant [-], D_0, D_p and D_s are the effective diffusivities [m^2/s] in bulk water, the porous media and the solid phase (in our case the cement paste). For Portland cement pastes, n≈ 2.7 and $\frac{D_S}{D_0}$ ≈ 2.0*10-4 (Oh et al., 2004). From literature, we know that the critical capillary porosity is approximately 0.18 (Garboczi et al., 1992).

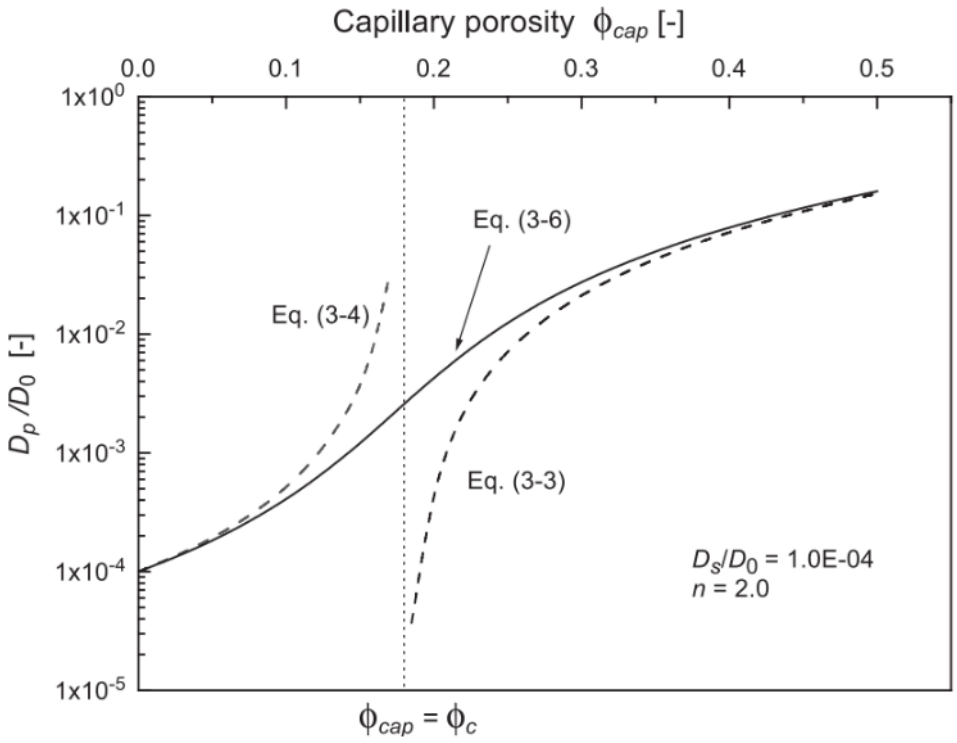

Figure 5 The conductivity through cement versus the capillary porosity. The vertical dashed line indicated the critical capillary porosity (0.18), and the solid line (labelled Eq. 3-6) shows the GEM equation(Oh et al., 2004).

The leaching of cement is a complex process is described through (1) a chemical model of cement as determined by mineral thermodynamics and (2) a diffusive transport module of the cement minerals which depends on the cement composition, minerals phases and cement microstructure. During leaching, there is feedback between the chemical cement composition and the diffusive transport as a result in changes in the cement porosity. Increasing porosity, due to mineral dissolution increases the rate of diffusion and results in a positive feedback by further increasing dissolution. However, mineral precipitation, for example the formation of protective calcite layers, decreases the porosity, which can decrease the diffusion rate. The system is complex and therefore must be modelled to quantitatively predict the changes in cement composition over time and the resulting rate of leaching.

2.3 Implementation

A cement model was implemented in the geochemical code PHREEQC 3.3.7, (Parkhurst et al., 2013), through the python package PhreeqPython (Vitens, 2021). CEMDATA07 was used, as described in section 2.2.2. The workflow for the model is shown in Figure 6.

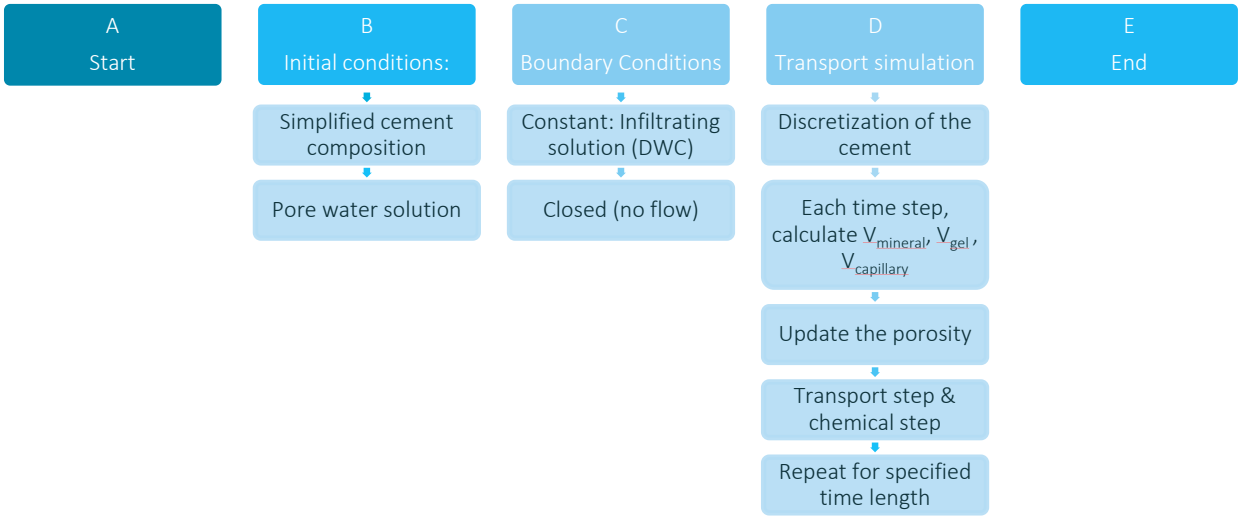

Figure 6 Workflow for the implementation of the cement model in PHREEQC.

First, a representative volume of cement is defined in PHREEQC. A subset of cement minerals were used in the model based on literature and the composition of OPC cement (Jacques, 2009). The equilibrium phases of the cement were as follows;

- 6 cement minerals: hydrotalcite, calcite, portlandite, monocarboaluminate, stratlingite, hydrotaliceOH,;
- 2 solid solutions: ideal solid solutions of jennite- and tobermorite-like CSH minerals and ettringite-tricarboaluminate
- 8 elements: Al, C, Ca, K, Mg, Na, S, Si.

The cement was created in PHREEQC by equilibrating the cement with water, using a w/c ratio of 0.5 (Elzenda et al., 1974; Eternit, 1980). Equilibrium of the cement with the pore water determines the composition of the pore water solution (B in Figure 6).

The boundary conditions (C in Figure 6) for the model were set as closed on the right side (Neumann type boundary condition), representing the outer walls of the cement pipe. It was assumed that negligible degradation of the cement pipe occurs from the outer pipe. The inner pipe wall (left boundary condition) was set as a constant concentration equal to the drinking water composition of interest (Dirichlet type boundary condition). Pipe wall thickness was set at 5 mm in the simulations with the four drinking water compositions.

The diffusion model was implemented as 1D, diffusive only transport using the TRANSPORT keyword in PHREEQC (D in Figure 6). We neglect electro-diffusive phenomena, consequently each aqueous species has the same diffusion coefficient (Jacques, Šimůnek, et al., 2011). Using the multi-component diffusion option in PHREEQC, overall charge balance is maintained (Parkhurst et al., 2013). Multicomponent diffusion also allows non-uniform porosity throughout the model, therefore changes in the mineral concentrations and associated changes in porosity were modelled as a function of depth.

To model the dual porosity of cement and the diffusion through both capillary and gel pores the GEM equation was used (Eq. 4 & Eq. 5, Oh et al., 2004) to describe diffusion. However, in PHREEQC, the relationship between porosity and diffusivity is hard-coded and it is not possible to implement a custom diffusion equation directly in the

TRANSPORT keyword block. It was assumed that cells contained only water and the pore water diffusion coefficient (D_p) for calculating the flux is;

$$D_p = \emptyset^n D_0 \qquad \textit{Eq. 6}$$

Where Ø is the porosity [-], *n* the Archie coefficient [-] and D_0 the pure water diffusion coefficient [m^2/s] (Appelo et al., 2005);

To simulate the dual porosity of the gel and capillary pores in PHREEQC using the GEM formula (Eq. 4 & Eq. 5), a pseudo-porosity value, termed here the GEM-porosity ($\emptyset_{GEM}$) was calculated from the GEM model as;

$$\emptyset_{GEM} = \mathrm{m}_\emptyset + \sqrt{m_\emptyset^2 + \frac{\emptyset_{ccp}}{1-\emptyset_{ccp}}\left(\frac{D_s}{D_0}\right)^{\frac{1}{n}}} \qquad \textit{Eq. 7}$$

Substituting $\emptyset_{GEM}$ into Eq. 6 gives;

$$\emptyset^n = \emptyset_{\mathrm{GEM}}^n \qquad \textit{Eq. 8}$$

$$D_p = \emptyset_{\mathrm{GEM}}^n D_0 \qquad \textit{Eq. 9}$$

This GEM-porosity was implemented using the built-in BASIC command program of PHREEQC to calculate the GEM-porosity after a specified number of time steps. To save computational time, the porosity was updated after each 100th time step. No difference was observed with performing the calculation after each time step versus after every 100th time step. The mineral phase, gel and capillary porosities were calculated using Eq. 11 - Eq. 18 (Appendix) for a volume fraction of the gel pores (φ_g) equal to 0.274, (Brouwers, 2004). During degradation of the cement, a decrease in the volume of the cement corresponded to an increase in the porosity (and vice-versa), decalcification of the CSH-gel did not change the capillary porosity, except due to changes in the volumes of the total amount of jennite and tobermorite, while changes in the CSH-gel corresponded to changes in the gel porosity.

2.4 Verification

2.4.1 Verification of chemical model of cement

Verification of a model checks that the operational and computational model are consistent. To verify the chemical model of cement, the simulations of chemical degradation of cementitious material for nuclear waste disposal was replicated (Jacques, 2009; Jacques et al., 2013, 2010; Jacques, Wang, et al., 2011). The cement phases included were;

- 17 cement minerals: Na_2O, K_2O, CAH_{10}, hydrotalcite, calcite, portlandite, gypsum, anhydrite, brucite, $Al(OH)_{3am}$, SiO_{2am}, monocarboaluminate, hemicarboaluminate, stratlingite, C_2AH_8, hydrotaliceOH, hydrogarnetOH;

- 3 solid solutions: ideal solid solution of jennite- and tobermorite-like CSH minerals and the non-deal solid solutions of Ettringite-tricarboaluminate and C_4AH_{13}, monosulfoaluminate;

The chemical model simulates the mineralogical changes in cement as it is exposed to successive pore volumes of water. Unlike the diffusive model, there is no feedback of loss minerals to the porosity, therefore the results are only qualitative.

The cement was equilibrated successively with 1 kg of water (Figure 7). After each equilibration, the water was replaced with a new mass of water, while the changes in the solid phase were carried forward to the next calculation. Therefore, the change in cement composition is reported as a function of the cumulative mass of equilibrated water. The solid phase was calculated using Eq. 11 and the total porosity was calculated from the model of Powers (Brouwers, 2004) for the given w/c ratio (0.5). In the static model gel and capillary porosity were not distinguished. As a result, a decrease in the volume of the cement corresponds to an increase in the total porosity (and vice-versa).

The model was verified for the five water compositions given in (Jacques et al., 2013), Table 3. The concrete model of Jacques was composed of 350 g OPC cement, as described in section 2.2.1, with a representative volume of 1000 cm^3, a w/c ratio of 0.5 and 1825 of calcite aggregate.

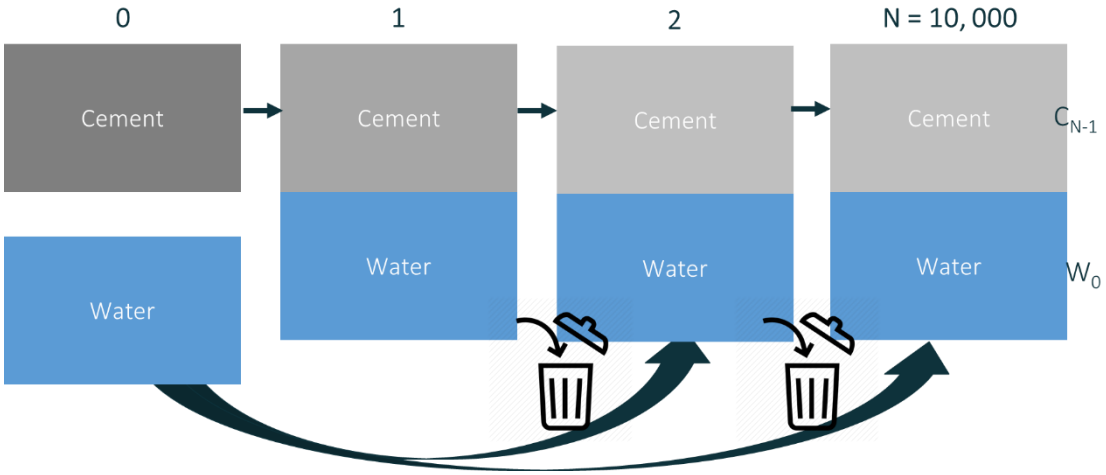

Figure 7 Conceptual model of the verification of the chemical model, where cement is brought into contact with successive volumes of water and equilibrated.

Table 3 Water compositions used to verify the model, from Jacques et al., (2013)

CASE	1	2	3	4	5
DESCRIPTION	Rain water wet only	Rain water bulk deposition	Soil water CO2	Soil water gibbsite	Soil water weathering
AL	0	0	0	1.02E-05	4.48E-05
C	1.70E-05	1.70E-05	2.67E-04	2.72E-04	2.70E-04
CA	5.00E-06	5.35E-05	5.35E-05	5.71E-05	5.71E-05
CL	5.12E-05	1.82E-04	1.82E-04	1.82E-04	1.82E-04
K	3.80E-06	2.94E-05	2.94E-05	6.53E-05	6.53E-05
MG	5.00E-06	2.27E-05	2.27E-05	2.53E-05	2.53E-05
N	1.17E-04	4.12E-04	4.12E-04	3.54E-04	3.54E-04
NA	4.40E-05	1.79E-04	1.79E-04	2.05E-04	2.05E-04
S	3.50E-05	1.19E-04	1.19E-04	1.19E-04	1.19E-04
PH	3.78	3.34	3.34	4.41	3.73
PCO_2	-3.50	-3.50	-2.30	-2.30	-2.30

The degradation model from Jacques et al. (2010) described four degradation phases, see Box 1.

Box 1. Degradation phases of cement

Phase I: is characterized by a pH > 12.5 and high concentrations of the surrogate phases Na_2O and K_2O, this phase is relatively short (~0.35 kg of water).

Phase II: portlandite is depleted from the cement. This phase is particularly important, as it is responsible for the major part of the loss of the strength of cement during leaching (Carde et al., 1999). Stage II lasts approximately 70 kg.

Phase III: is the most mineralogically complex, ending after the depletion of the AFt, AFm and CSH-phases (see section 2.2.1). The pH of the pore water decreases to between 10-12.5 and ends after 1700 kg of water per 1000 cm^3.

Phase IV: OH-hydrotalcite and calcite are present with a pH below 10, the end of phase IV is the complete dissolution of calcite.

Results of verification

In four out of five cases, we had excellent agreement between the simulated and published model results. The total length of the different phases of cement degradation were within ± 5% of the published model results (Table 4), with the exception of Case 4. The model was not able to simulate the $Al(OH)_3$ peak in Case 4. We do not know why this mineral was not simulated in this case, but was simulated in cases 3 and 5 (Figure 22 and Figure 24).

Table 4 Length of cement phases in kg of water for the four solutions, where A are the simulations performed by our model and B are the published results used to verify the mode (Jacques et al., (2013))

CASE	1		2		3		4		5	
PHASE	A	B	A	B	A	B	A	B	A	B
1	0.35	0.35	0.35	0.35	0.35	0.35	0.35	0.35	0.35	0.35
2	73.5	72.0	72.5	72.0	71.5	71.0	72.5	70.0	71.5	70.0
3	1692.5	1766.0	1450.5	1520.0	1125.5	1162.0	1325.5	1185.0	1170.5	1203.0

The results for water composition 1 are shown in Figure 8, the remaining results are found in the appendix (Figure 21- Figure 24). The figure shows from top to bottom, (A) the pH for the solution in Case 1 (Rain water wet only) as a function of the total mass of water brought into equilibrium with the volume of cement. The pH decreases from a maximum initial value of 13.8 to a minimum value of 9.4 after 10, 000 kg of water. The concentration of elements in the water and the mineral concentrations are shown in Figure 8 B and C respectively. Finally the change in the solid phase (red line) and porosity (blue line) are shown in Figure 8 D.

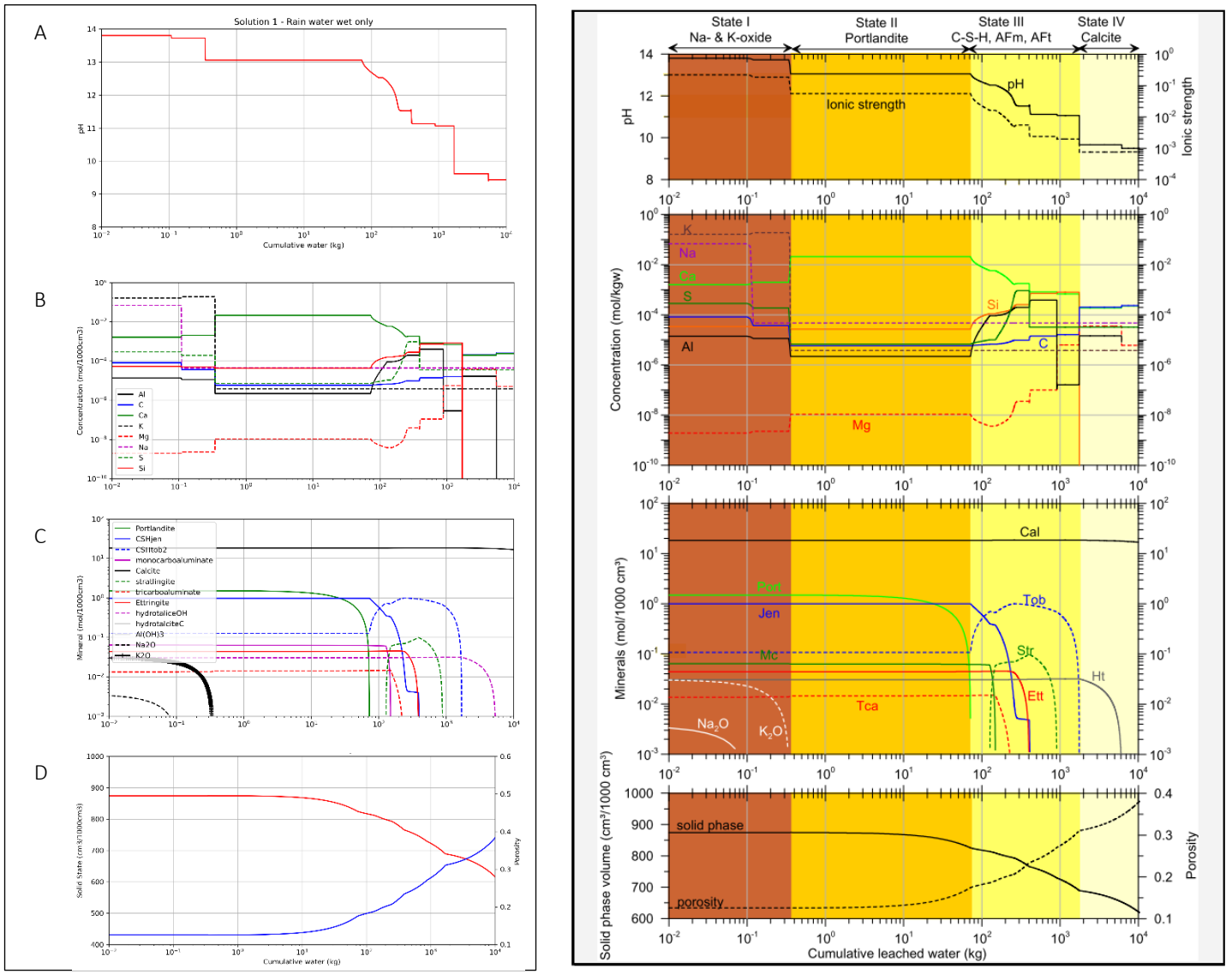

Figure 8 Left, results of the chemical model of leaching of 1000 cm³ of OPC with rain water (water composition 1) at 10°C. Results verified against the model of Jacques et al. (2013), right both visually for the different mineral concentrations and the total length of the different phases were compared in Table 4.

2.4.2 Grid independence

Grid independence is important as the solution of the differential equations for diffusive transport should be independent of the solution method. The grid in this case is the cell size, in mm. This is shown by varying the model cell size until the results no longer change meaningfully with a smaller grid size. Five different cell sizes were modelled: 0.0625, 0.125, 0.25, 0.5 and 1 mm using pure water as the infiltrating solution. As seen in Figure 9**Error! Reference source not found.**, the results of the portlandite front and the pH do not change meaningfully below a grid size of 0.125 mm. However, to balance the accuracy of the solution and the simulation time, a grid size of 0.25 mm was chosen for simulations for drinking water compositions.

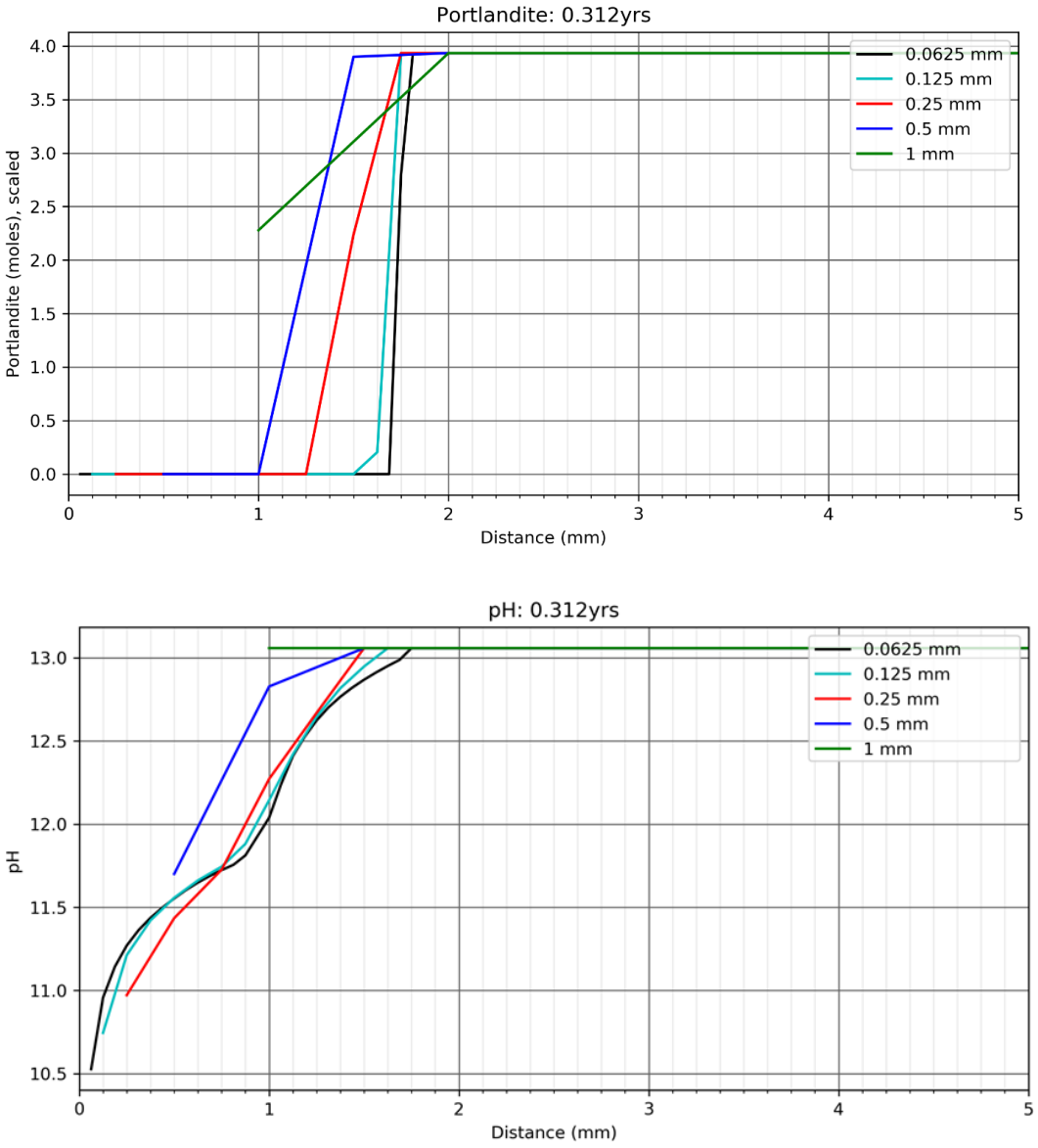

Figure 9 Grid independence simulations for A. Portlandite and B. pore water pH, shown after 114 days (0.312 years). With decreasing grid size, the depletion front for portlandite become sharper and the change in pH between cells smoother.

3 Validation of diffusion model from literature

To assess the accuracy and reliability of the model we validated the model against data from experiments of cement leaching described in the literature. Model validation is an important step in model development as it tests whether the model can accurately and reliably predict the behaviour of the system of interest. For our purposes, the behaviour of interest is the leaching of cement over time and the associated changes in the cement composition and leaching fronts. Validation from literature is a simple first step, while validation from practice, though also valuable and necessary, is more complex. This is because the experiments from literature are conducted under known, controlled conditions and readily available.

The diffusion model was validated from literature using the experiments of Moranville et al. (2004). These experiments were chosen as the set-up was relatively simple, the results clearly reported and the variables relatively easily implemented in our model. The set-up was blocks (30x20x20 mm) of OPC cement suspended in a flow-through cell with a refreshing rate of 1 L /day. Leaching rates were reported after 114 days as the mm of leached depth. The variables altered in the experiments were the aggressive solution (pure water and mineral water) and the w/c ratio, both of which were implementable in our model.

3.1 Method

In the experiments, three w/c ratios (0.25, 0.4 and 0.5) and two water compositions (pure water and mineral water, Table 5) were used. The cement paste in the models (CEM I 52.5N) was slightly different from the cement used (CEM I 42.5N), see Table 6. The cement paste also contained no aggregate, therefore the weight fraction of asbestos was set to zero in the simulations.

Table 5 Mineral water composition used in the validation of the diffusion model (Moranville et al., 2004).

	VALUE	UNIT
CA	11.5	mg/L
SI	31.7	mg/L
MG	8	mg/L
NA	11.6	mg/L
K	6.2	mg/L
CL	13.5	mg/L
SO_3	8.1	mg/L
HCO_3	71	mg/L
PH	7	[-]

To model the variations in the w/c ratio, the capillary porosity was calculated using the Powers model (Eq. 18) assuming full hydration of the cement (α=1), and the gel porosity was calculated as a fixed fraction of the CSH-gel (Eq. 16). The temperature was set at 26 °C (as in the experiments from the literature), pure water was taken as water at pH 7 with no other elements and the mineral water composition was given in Moranville (2004, Table 5). The experiments were conducted with mineral water with a w/c ratio of 0.4 and pure water at three w/c ratios (0.25, 0.4 and 0.5) for a period of 114 days (0.312 years). The leached depth (mm) was determined visually by the authors, as the depth of portlandite depletion. A finer grid (0.125 mm) was used in the validation simulations because the simulation times were much shorter (0.314 yrs vs 7 years) than for the drinking water simulations.

Table 6 Difference in composition of CEM I used in the validation and the value from literature.

	CEM I 42.5 N	CEM I 52.5 N
MINERAL	g/100 g OPC	% mass
CAO	62.4	67.4
SIO_2	18.9	23.4
AL_2O_3	4.4	3.05
FE_2O_3	2.5	2.15
CAO (FREE)	0.6	
MGO	1.4	0.7
K_2O	0.95	0.15
NA_2O	0.1	0.1
CO_2	2.1	
SO_3	3	2.1
ALITE (C_3S)	58	71
BELITE (C_2S)	10	13
ALUMINATE (C_3A)	7.6	4
FERRITE (C_4AF)	7.5	8
GYPSUM		3.5
LIMESTONE		2.5

3.2 Results and Discussion of Validation

The model simulated the leached depth of the cement for the mineral water case (w/c =0.4, Figure 10) and pure water (w/c =0.5, Figure 11Figure 10C) within 25% and 5% of the leached depth (Table 7). However, the simulations for the pure water scenarios with w/c of 0.25 and 0.4 (Figure 11 A, B) had larger differences between the experimental simulation values, underestimating the leached depth by about 80% (Table 7).

Table 7 Leached depth (mm) of experiments from literature and simulations

	LITERATURE		SIMULATION	
W/C	Pure water	Mineral Water	Pure water	Mineral Water
0.25	0.8 ± 0.1		0.125	
0.4	1.5 ± 0.1	<0.3	0.375	0.375
0.5	1.8 ± 0.1		1.75	

The deviation of the model for the two lower w/c ratios may be due to a number of reasons. Deviations from the porosities of the paper may account for some of the deviation of the simulation results from the experimental results. Since the gel porosity was still tied to the CSH volume, while the capillary porosity was calculated from the Powers model, the total porosity of the simulations differed from the total porosities measured in the paper (Table 8). The authors did not report the gel and capillary porosities separately, so it was not possible to verify the gel and capillary porosities separately.

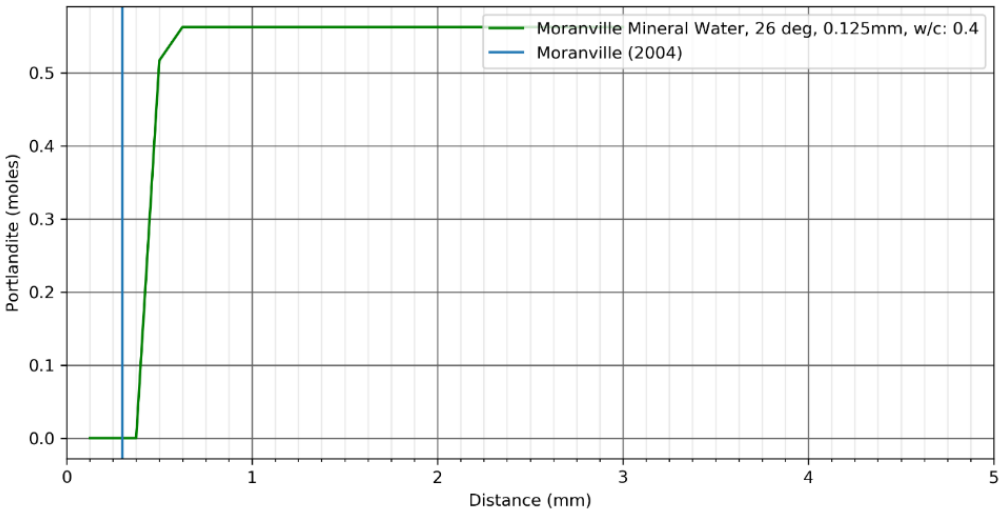

Figure 10 Portlandite depletion (as proxy for leached depth) for mineral water at a w/c of 0.4 at 26 °C. The green line shows the moles of Portlandite per cell (cell size in light grey grid) and the blue line shows the leached depth (mm) from experiment from literature.

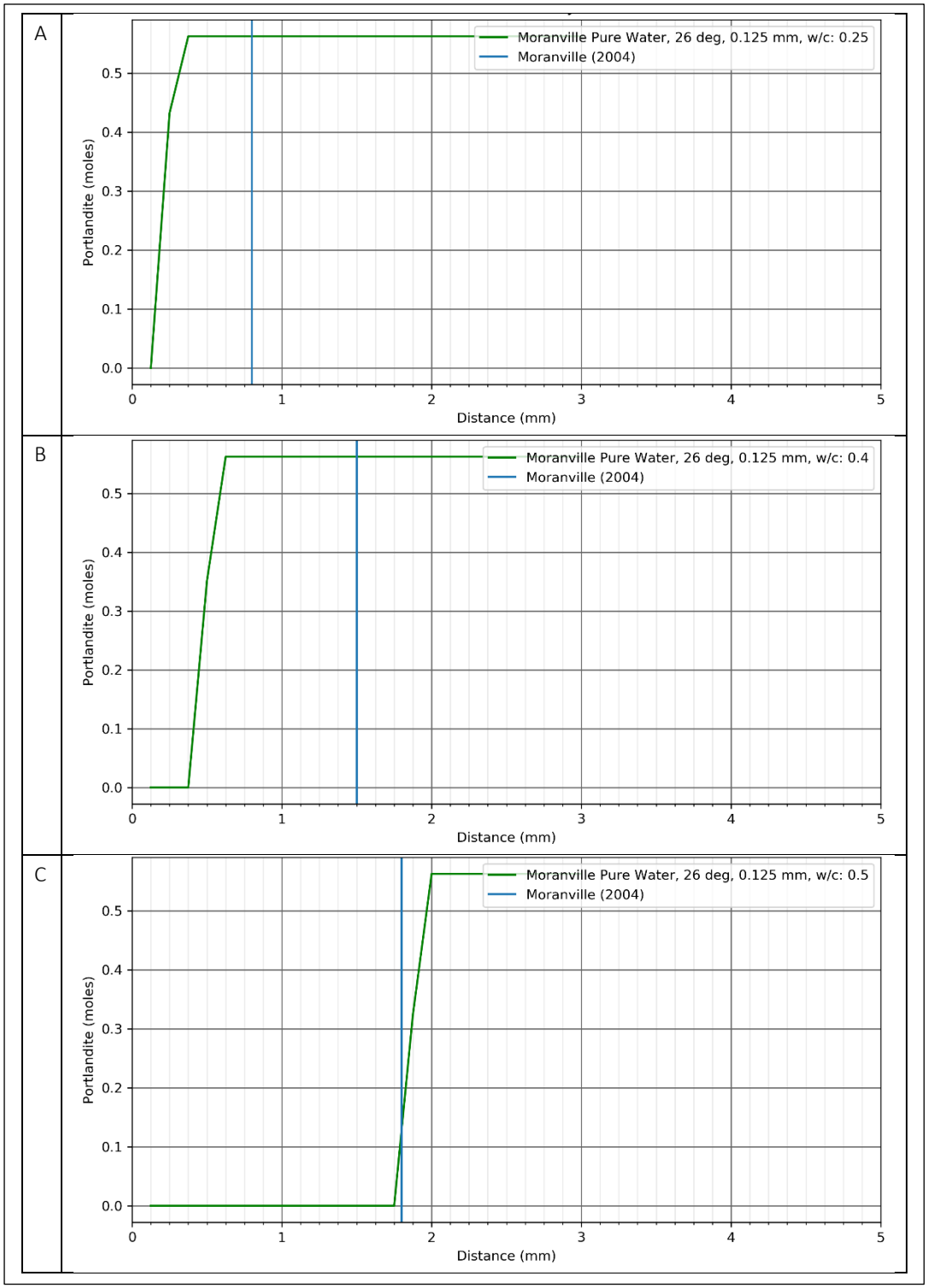

Figure 11 Portlandite depletion for pure water at a w/c of 0.25 (A), 0.4 (B) and 0.5 (C) at 26 °C. The green line shows the moles of Portlandite per cell (cell size in light grey grid) and the blue line shows the leached depth (mm) from experiment from literature.

In addition, in the model, the critical capillary porosity of 0.18 was used (Garboczi et al., 1992). However, some variation in the critical capillary porosity has been found (Sant et al., 2011), and the critical capillary porosity may be influenced by the w/c ratio, the curing time, cement type etc. (Hu et al., 2005). The critical capillary porosity is important as further the initial capillary porosity is from this value, the slower the diffusion. Finally, the cement composition of the experiments was slightly different (CEM I 52.5N vs. CEM I 42.5 N) than used in the model, which

may result in slightly different distributions of the gel/capillary porosity, and therefore diffusive behaviour. In a follow up project the sensitivity of the model for the gel, capillary and critical capillary porosity will be examined in more detail. Further validation of the model from literature and practice will also be performed.

Table 8 Total porosity (%) of the validation experiments from literature and the calculated total porosity from the simulations

W/C	LITERATURE	SIMULATION
0.25	25	33.3
0.4	39	31.9
0.5	44	40.2

4 Drinking water simulations

4.1 Adaptations of the chemical model from concrete to asbestos cement

In our simulations we use asbestos cement, therefore the calcite aggregate used in the simulations of Jacques et al., (2013) was removed and replaced by (inert) asbestos. The w/c ratio was kept at 0.5, for a final cement composition with 10% asbestos, 60% cement and 30% water from the literature (Elzenda et al., 1974; Eternit, 1980). The asbestos volume was calculated by assuming chrysotile asbestos, with a density of 2.53 g/cm^3 (Pundsack, 1956). The cement composition was rescaled to have a final cement volume of 1000 cm^3, the representative volume used in the previous simulations (Table 9). The mineral phase composition of the cement was then rescaled to the calculated initial mass of OPC used.

Table 9 Rescaling of cement composition to account for the change from concrete to asbestos cement

	Mass (g)	Initial Mix (%)	Volume (cm^3)	Scale to 1000 cm^3	Mass initial mix (g)
Asbestos	58.3	10	23	63.25	160.04
OPC	350	60	198.5	556.12	960.25
Water	175	30	-	-	480.13
Pore Volume	-	-	142.2	380.6	-
Total	-	100	363.7	1000	-

4.2 Selection of drinking water compositions

Four locations from a selection of drinking water compositions were chosen in consultation with representatives from each of the four drinking water companies. The four locations were chosen to have compositions which represent water which regularly does not meet the DWB (drinkwaterbesluit, labelled *problematic*), which sometimes does not meet DWB (*sometimes problematic*) and which does not have any problems (*not problematic*, see Box 2). Further, the compositions were chosen to have a range in concentrations for trace elements (Table 10).

Box 2. Selection of drinking water locations

Lekkerkerk (Oasen): *Sometimes problematic* - Location with partial flow RO (50%). Structurally SI <0, boiling tests also completely 0. Regularly also SI <-0.2.

Nijverdal (Vitens): *Problematic* - SI does not meet the Drinking Water Directive, however aggressive CO_2 does meet the German standard, TAC relatively low.

Andijk (PWN): *Problematic* - History water quality with, among other things, a high corrosion index (2-3) and new pre-treatment (more chloride, less sulphate) operational since 2019 which supplies water in partial flow to the drinking water via post-purification.

Hoogeveen (WMD): *Not problematic*

Table 10 gives average the composition of the water qualities from each location. As the water qualities given were average concentrations, the saturation index (SI) of calcite and the partial pressure of CO_2 were recalculated by PHREEQC. These are reported in the bottom of the table.

*Table 10 Composition of drinking water from four locations. Data given are average values for water composition in units of mol/ kgw unless otherwise indicated). The average values for the CO_2 and SI are reported (indicated by *) but were recalculated by PHREEQC for the given averaged values and the recalculated values were used in the simulations.*

	OASEN LEKKERKERK	VITENS NIJVERDAL	PWN ANDIJK	WMD HOOGEVEEN
Al	2.19E-07	4.84E-08	4.20E-08	2.96E-07
Ca	1.08E-03	7.46E-04	8.50E-04	1.10E-03
C	1.48E-03	3.86E-04	4.54E-03	8.18E-04
K	5.75E-05	3.05E-05	0.00E+00	4.60E-05
Mg	5.67E-09	1.18E-04	5.29E-04	3.33E-04
N	1.85E-07	1.35E-04	7.11E-05	2.57E-05
Na	1.43E-03	4.77E-04	5.48E-03	8.26E-04
S	2.75E-04	2.56E-04	8.41E-04	0.00E+00
Fe	4.57E-08	1.70E-08	3.59E-08	5.37E-08
Si	1.32E-04	2.51E-04	5.32E-05	4.27E-04
pH [-]	7.83	7.87	8.16	8.20
Temperature (°C)	12.95	10.13	11.29	11.50
Alkalinity	3.00E-03	1.68E-03	3.12E-03	3.93E-03
CO_2*	5.74E-05	1.89E-05	2.91E-05	1.31E-05
SI* [-]	-0.08	-0.41	0.11	0.58
Phreeqc calculations				
CO_2 (atm)	$10^{-2.65}$	$10^{-2.95}$	$10^{-3.00}$	$10^{-2.92}$
SI [-]	0.11	-0.27	0.26	0.58

4.3 Mineralogical evolutions when exposed to drinking water results

To asses the influence of water composition in the absence of the effects of diffusion, first the mineralogical evolution of cement as a function of drinking water composition were modelled using the chemical model of cement (see section 2.4.1). This allows us to isolate the effect of chemical equilibrium from the effects of the feedback of mineral dissolution/precipitation on diffusion. The chemical evolution was modelled for 20,000 kg of water, using a representative volume of 1000 cm^3 of asbestos cement (see section 2.4.2) and a w/c ratio of 0.5. For one water composition, Lekkerkerk (Oasen), the simulation was extended to 200,000 kg of water to observe the longer term effect on the $Al(OH)_3$ and calcite behaviour. Due to convergence issues, the cement composition was simplified for the Hoogeveen (WMD) composition. The behaviour of the simplified cement composition was verified by modelling the Lekkerkerk (Oasen) drinking water compositions using both the full and simplified composition and comparing the length of the three different phases. Phase lengths were found to be within 1% of the full case and are therefore representative. Phase 4 is not shown since phase 4 only ends after the complete dissolution of calcite, which in cases where there is a positive SI, does not occur and in the case of a negative SI, requires more than the 10,000 kg of water added.

Results

The chemical evolution of the four cases were found to be comparable to the phases described by Jacques et al., (2013), see Box 1 on page 18. The first two phases were relatively insensitive to the water composition (Figure 12). In the first phase, defined by the loss of the surrogate phases Na_2O and K_2O, the difference between the least and

most amount of water to end the phase was 13 % (0.11 kg of water). In the second phase, defined by the loss of portlandite, the difference was 5% (8 kg). Nijverdal (Vitens) took the most volume of water, at 178 kg, while Andijk (PWN) and Hoogeveen (WMD) requires the least amount of water deplete the portlandite. Similarly, during the third phase, the water required to end the phase for the different water compositions from most to least water were: Nijverdal (Vitens) > Lekkerkerk (Oasen) > Andijk (PWN) > Hoogeveen (WMD). The difference in water volume between the most and least was 40% (854 kg).

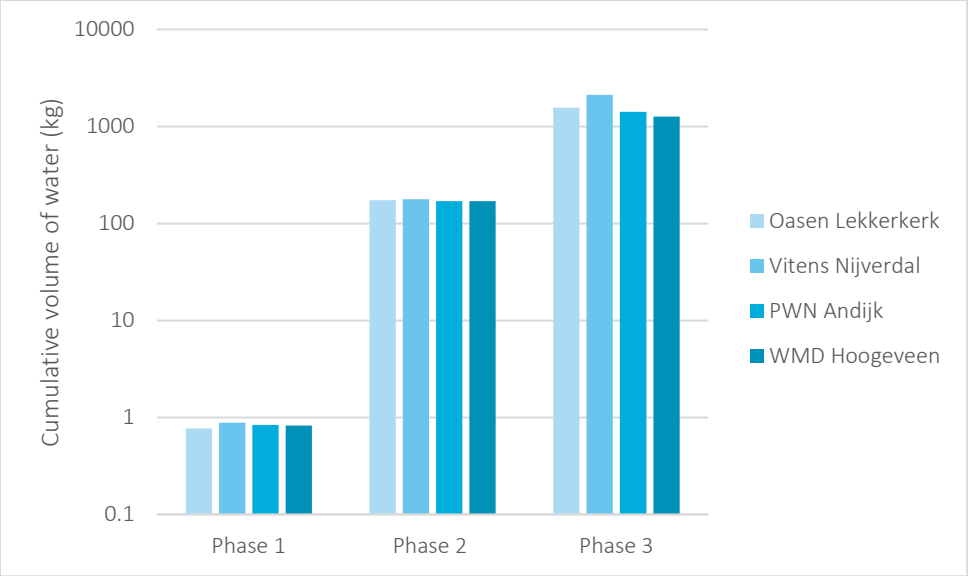

Figure 12 Cumulative volume of water to end each of the first three phases for the four drinking water compositions. For WMD Hoogeveen the third phase length was calculated using the simplified AC composition.

However, the length of the phases does not capture the complete behaviour of the system, and it is also important to consider the behaviour of calcite for the different water compositions (Figure 13). The water compositions with a positive SI for calcite (Oasen, PWN and WMD) precipitated of calcite, while Vitens, with a negative SI initially precipitated of calcite during the first three phases but then calcite was dissolved in the fourth phase. The precipitation (or dissolution) concentration mirrors the SI of the water composition, with the highest precipitation concentration for WMD (SI: 0.58, precipitation concentration: 1.56E-04 mol/kgw), followed by PWN (SI: 0.26, precipitation concentration: 4.87E-05 mol/kgw) and Oasen (SI: 0.11, precipitation concentration: 2.74E-05 mol/kgw). Vitens, the only water composition with a negative SI shows the dissolution of calcite in the fourth phase (SI: -0.27, dissolution concentration: 3.24E-05 mol/kgw).

Therefore, as expected, in the chemical model, the magnitude and the sign of the SI predicted the precipitation/dissolution behaviour of the calcite: a negative SI corresponded with the dissolution of calcite; while a higher, more positive SI corresponded with more precipitation of calcite per kg of equilibrated water. The length of the third phase, the most mineralogically complex phase, also varied with the water composition, but with an inverse relationship to what we expected. We observed that more water was required to end phase three for water compositions we expected to be less aggressive (e.g. positive SI), while the opposite was true for more aggressive water (negative SI, longer third phase). We do not yet know why this occurs and therefore cannot speculate as to the reason for the difference in the length of the third phase.

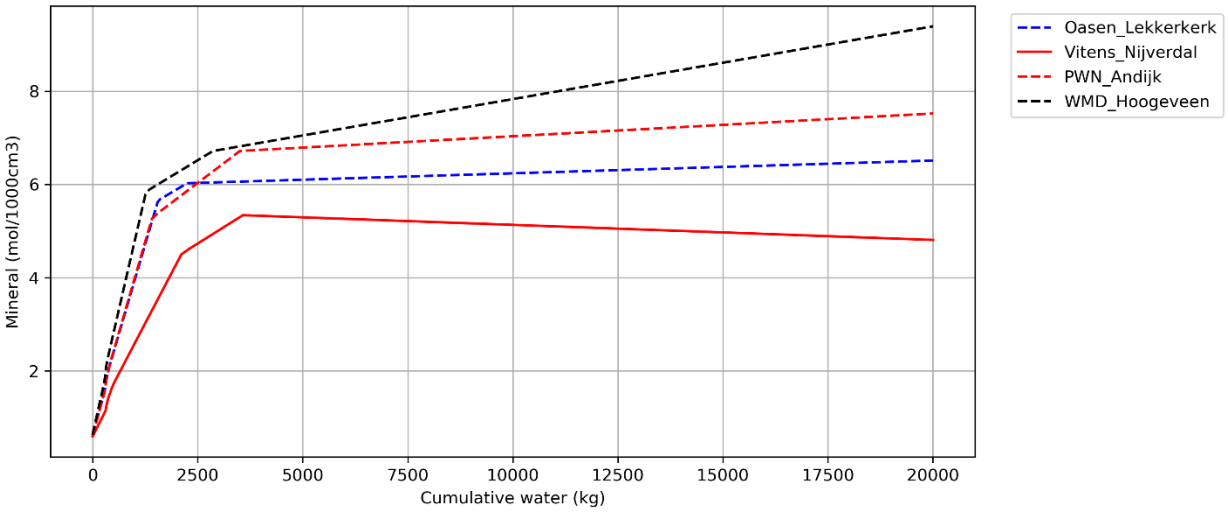

Figure 13 Behaviour of calcite in the final phase of chemical evolution for the four drinking water compositions. Water compositions with a positive SI (Oasen, PWN, WMD) show precipitation of calcite, while a negative SI (Vitens) shows the dissolution of calcite

4.4 Effect of drinking water composition on leaching rates

To calculate the leaching rates in asbestos cement pipes, the diffusion model was simulated using the same four water compositions in the chemical model. Simulations were performed for 7 years with a cell size of 0.25 mm for a 5 mm thick pipe wall section. Only the first 5 mm of the pipe were modelled to optimize the simulation time and because the length of the pipe behind the leaching front does not influence the cement in before the leaching front. This model does not take into account the effects of changes in water composition along a pipe. This will be explored in follow-up projects.

Results

Substantial differences were found for the different drinking water compositions within the first few years of simulation. Both the Andijk (PWN) and Nijverdal (Vitens) had complete depletion of portlandite within the first 5mm during the simulation. For Andijk, the first 5mm were depleted within 4.25 years, while for Vitens the first 5mm were depleted with 5.53 years (Table 11). In contrast, portlandite was still present in Lekkerkerk (Oasen) and Hoogeveen (WMD) after 7 years. The portlandite depletion front for Lekkerkerk was between 1.75-2 mm, while for Hoogeveen it was between 3.5-3.75 mm (Figure 14).

Table 11 Leached depth over time for the four drinking water compositions. Leached depth determined as the depth of portlandite depletion.

LEACHED DEPTH (MM)	TIME (YEARS)			
	PWN	Vitens	WMD	Oasen
0.25	0.04	0.03	0.03	0.03
0.5	0.10	0.09	0.08	0.10
0.75	0.19	0.18	0.15	0.23
1	0.30	0.30	0.25	0.54
1.25	0.43	0.45	0.37	1.17
1.5	0.58	0.63	0.54	2.36
1.75	0.75	0.84	0.75	4.38
2	0.92	1.08	1.03	
2.25	1.12	1.34	1.37	
2.5	1.32	1.63	1.81	
2.75	1.54	1.93	2.38	
3	1.77	2.26	3.11	
3.25	2.02	2.60	4.09	
3.5	2.29	2.97	5.35	
3.75	2.57	3.35		
4	2.87	3.75		
4.25	3.19	4.17		
4.5	3.53	4.61		
4.75	3.88	5.06		
5	4.25	5.54		

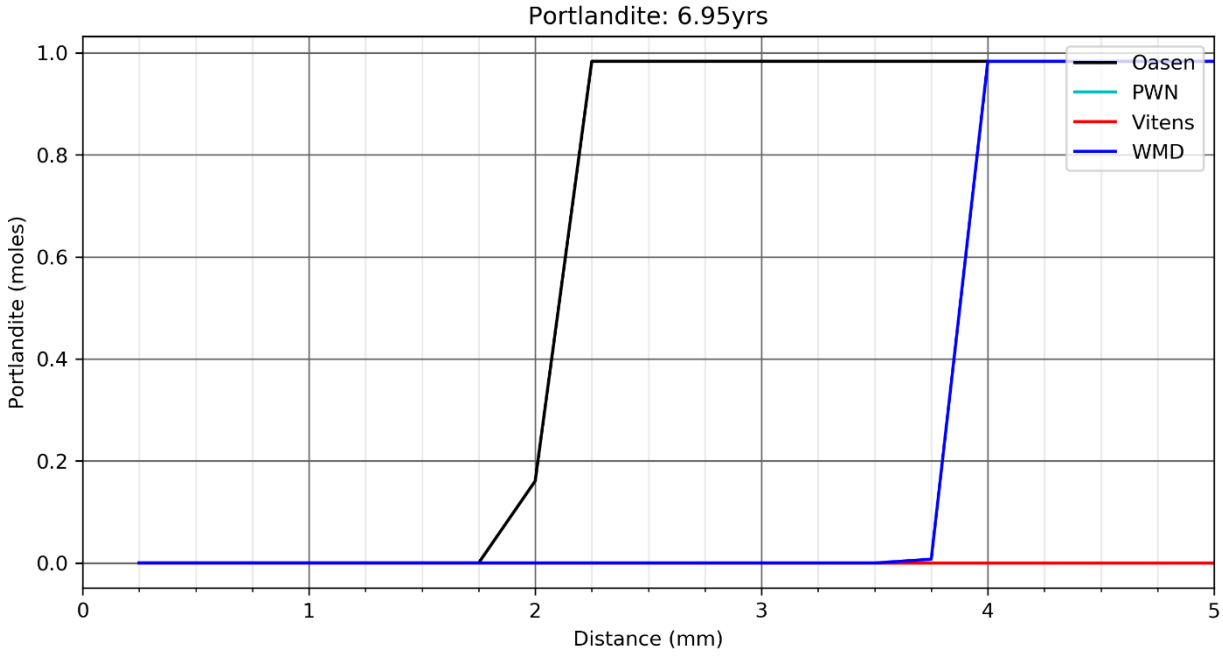

Figure 14 Portlandite depletion fronts for the four water compositions after 7 years simulation as a function of depth into a simulated 5 mm pipe wall. Vitens and PWN show complete portlandite depletion. Cell size (0.25 mm) shown as light grey grid on x-axis.

For purely diffusive processes, the rate of degradation is proportional to the square root of time, so long as the cement is homogenous and there are no changes in the incoming water composition (Mainguy et al., 2000). For these conditions, the degradation has been shown to be linear with the square root of time (Moranville et al., 2004), and from the steady-state value, the depth of leaching can be predicted for any length of time. The rate of leaching is expressed in terms of a Boltzman transformation (λ):

$$\lambda = x\sqrt{t} \qquad \textit{Eq. 10}$$

Where x is the leached depth (portlandite depletion) and t is the time in years. From Figure 15 it is seen that for the water composition from PWN and Vitens, the leached depth is approximately linear with the square root of time, as expected for a purely diffusive process (Mainguy et al., 2000). However, for Oasen and WMD, the leached depth differs from linear, as a result of the changed in porosity and therefore diffusivity, due to calcite precipitation.

Figure 17 shows the progressive decrease in cell porosity at the left boundary for both Lekkerkerk (Oasen) and Hoogeveen (WMD). The decreased cell porosity restricts the diffusion of water to deeper cells, decreasing the portlandite dissolution, resulting in the decreased portlandite leaching rate. The decreased cell porosity is primarily due to the precipitation of calcite (see section 4.5). Similarly, we can see that leaching for the water composition from PWN is faster due to lower porosity. The changes in porosity cause the deviation from predicted linear with square root of time for the degradation of the cement. Possibly given a longer simulation time, a steady state may be reached for Oasen and WMD, which would allow for the prediction of the leached depth for any length of time.

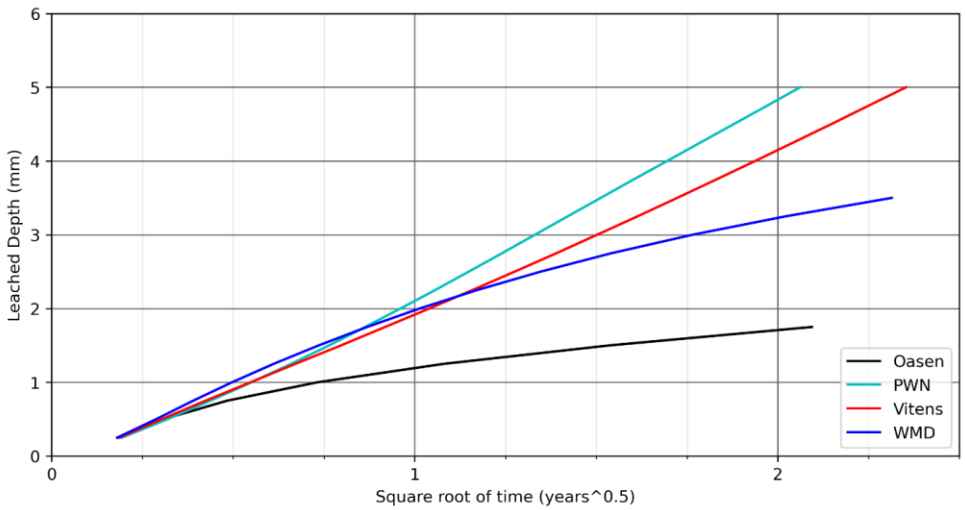

Figure 15 The depth of degradation versus the square root of time for degradation for each water composition. The depth of degradation for purely diffusive processes is linear with the square root of time. This holds for the water compositions of PWN and Vitens. However, for WMD and Oasen, the trend differs from linear as a result of the precipitation of calcite, resulting in decreased porosity, and therefore diffusivity over time.

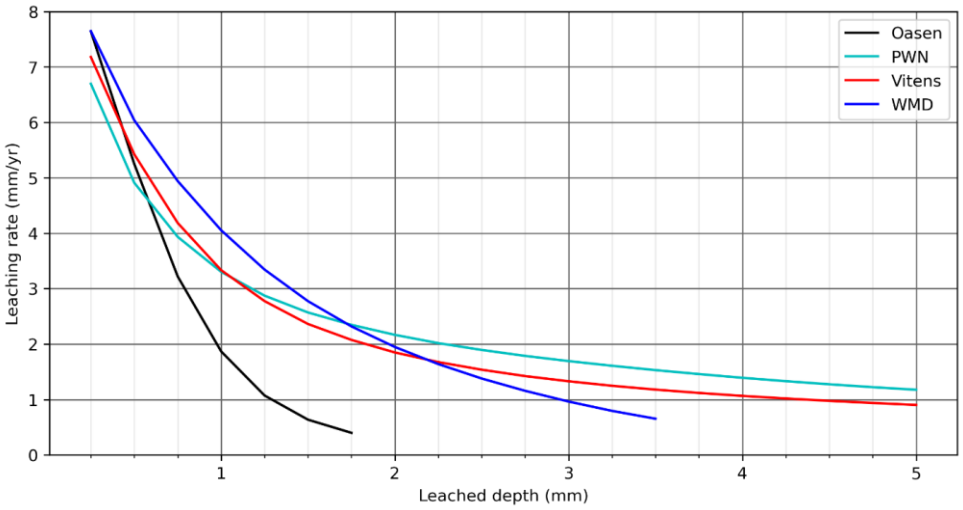

Figure 16 Leaching rate (mm/yr) as a function of degraded depth in the cement pipe. The rate of leaching decreases with depth for all water compositions, though the rate does not yet reach a steady-state

Figure 16 shows the leaching rate (mm/yr) as a function of the leached depth in the cement pipe. Each water composition shows a decreased in the leaching rate with depth though a steady state rate has not yet been reached. The leaching rates of degrading pipes in practice typically vary around 0.05 mm/year up to at most 0.3 mm/year, based on extensive exit assessments performed by Brabant Water, as described in (van Laarhoven et al., 2019). The leaching rate for the water compositions decreases with depth for all water compositions, with the lowest leaching rate for Oasen (0.4 mm/yr), and the highest for PWN (1.18 mm/yr). Therefore the model leaching rate is higher for all compositions compared to practice. The reason for the elevated leaching compared to practice will be explored further in the follow-up project, through a systematic sensitivity analysis and through validation of the model from practice.

The substantial differences in the leaching rates for the different water compositions is in contrast to the relative insensitivity of the chemical model of cement to the different water compositions. At most, a 40% difference in the mass of water to end the third phase was observed between the different water compositions. For the diffusion model, we observe a 68% difference in the leached depth of Portlandite after 4 years for the different compositions (Table 11). This is due in large part to the feedback of the precipitation of calcite on the porosity, and therefore diffusivity, of the cement.

4.5 Effects of drinking water composition on scaling

Precipitation of calcite was observed for each of the four water compositions, however, only Lekkerkerk (Oasen) and Hoogeveen (WMD) showed persistent calcite deposition at the left boundary (in contact with the drinking water, Figure 18). The calcite precipitation in the Lekkerkerk and Hoogeveen simulations in the left-most cells resulted in decreased cell porosity and therefore decreased leaching of, among others, portlandite.

Interestingly, the SI of the water composition is not the sole predictor of the precipitation rate of calcite or the leaching rate in the diffusion model. This is in contrast to the results of the chemical model (with no feedback of the mineralogical changes in the cement to the porosity), where the SI determined the rate of calcite precipitation (or dissolution) in the fourth phase (section 4.3). Based on the SI alone, we would expect Hoogeveen (WMD) to have the highest precipitation rate for calcite and for Andijk (PWN) to also precipitate calcite, and at a rate higher than that of Lekkerkerk (Oasen). However, we observe greater calcite precipitation for the water composition of

Lekkerkerk than for Hoogeveen, though the SI for Hoogeveen is 0.58 compared to 0.11, and no sustained calcite precipitation for Andijk (SI 0.26).

The model shows that SI alone does not predict leaching in the cement and that there is a complex relationship between the leaching of cement and water composition. In a follow up project, the relationship between leaching behaviour and index parameters (e.g. Calcium Carbonate Precipitation Potential (CCPP), aggressive CO_2) will be explored in more detail. In addition, the model assumes that calcite deposition results in decreased porosity of the cell in which calcite is precipitated. The exact relationship between calcite deposition and the porosity will also be investigated in the follow-up project. Currently, the precipitation of calcite increases the solid phase in the cell, which decreases the porosity.

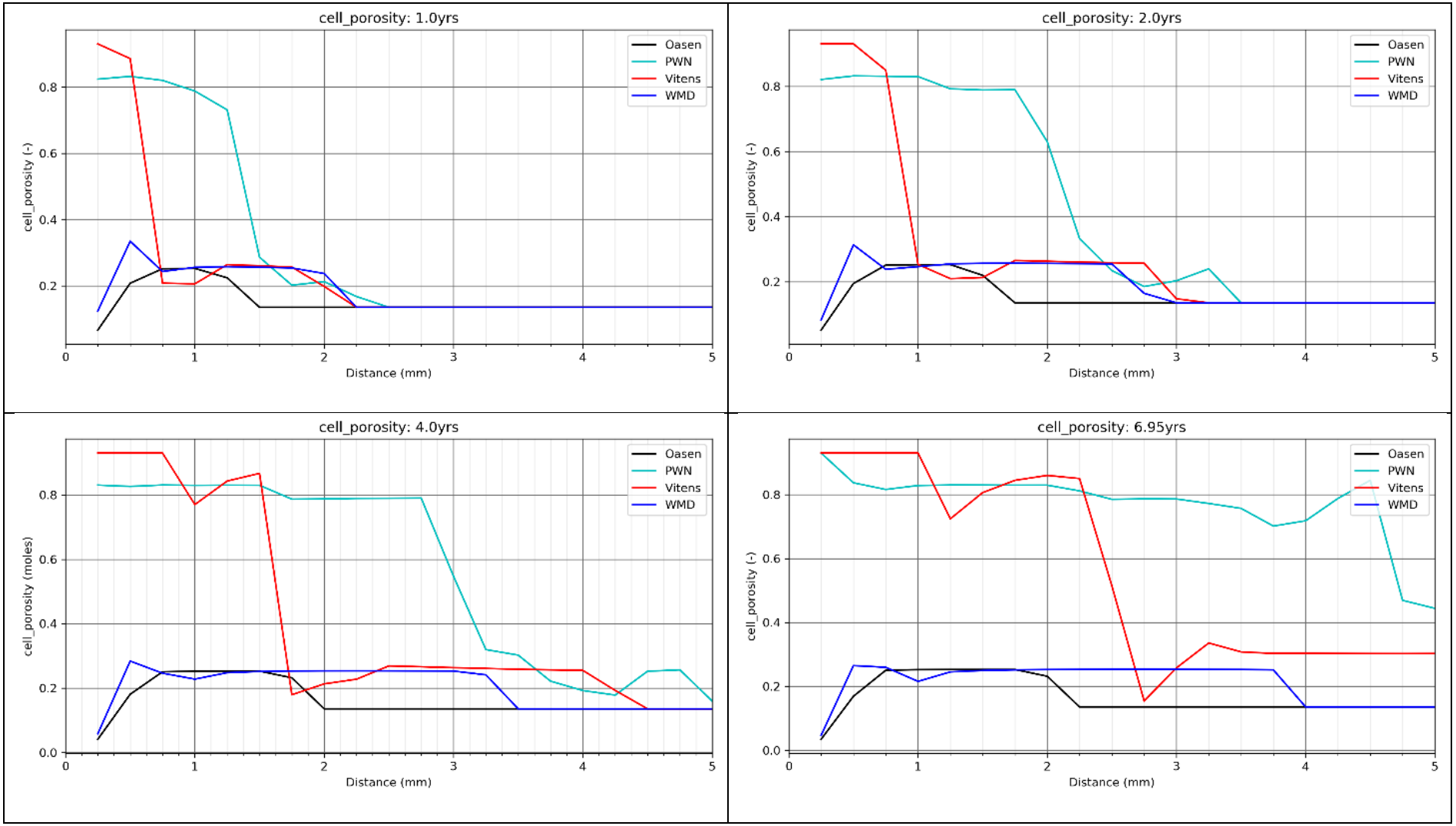

Figure 17 Development of porosity over time for the four water compositions as a function of depth after 1, 2, 4 and 6.95 years. Oasen and WMD show restricted cell porosity in the first cell, due to calcite precipitation, while PWN and Vitens show complete mineral depletion in the first cell after 6.95 years

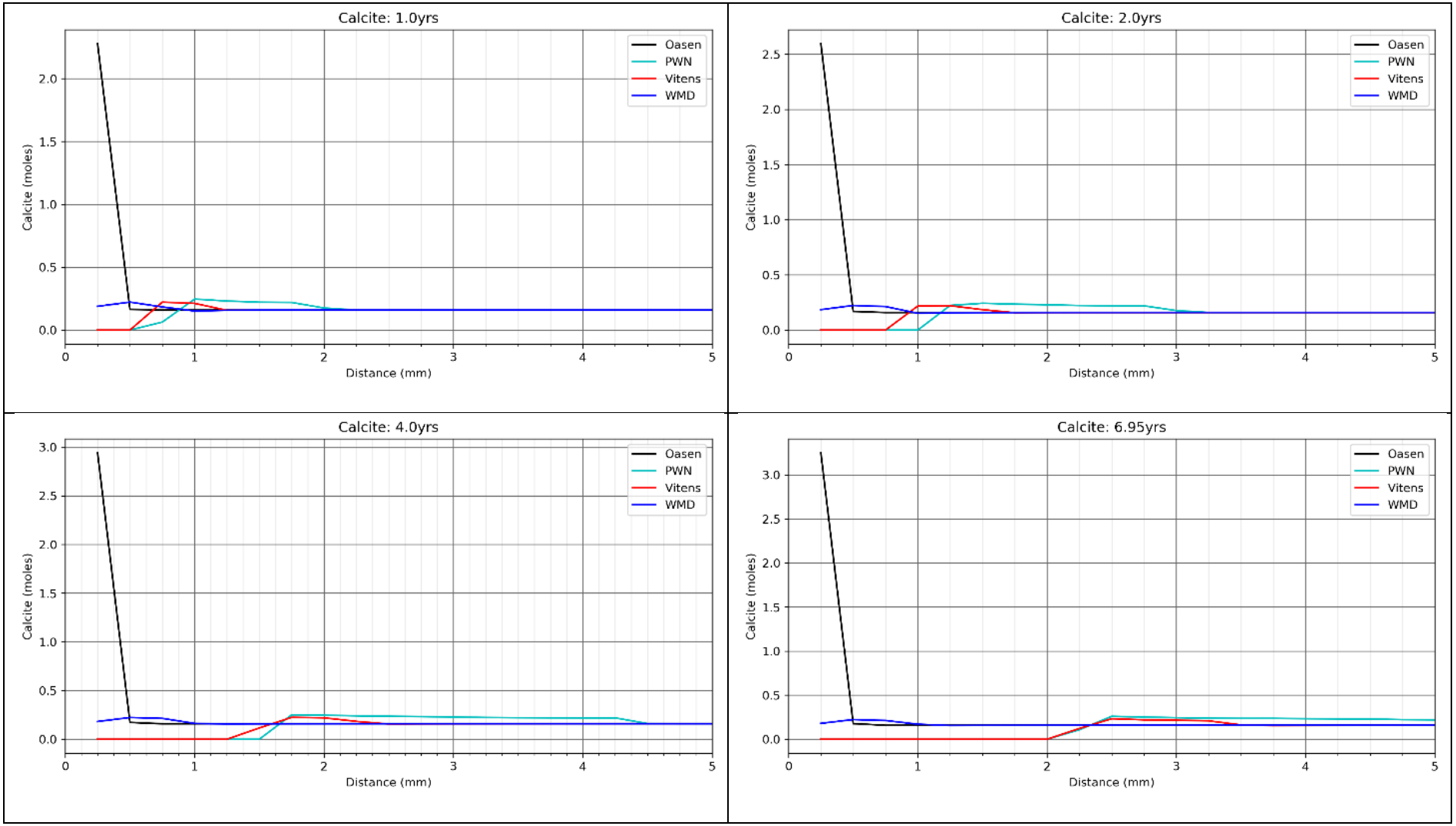

Figure 18 Moles of calcite as a function of depth for the four water compositions after 1, 2, 4 and 6.95 years. Note the increasing y-axis over time, showing the precipitation of calcite in the left-most cell (in contact with the drinking water) for Oasen.

5 Discussie, conclusies en aanbevelingen

5.1 Discussie

Een model om de chemische veranderingen en de tijdschaal van uitloging in cementhoudende drinkwaterleidingen te voorspellen is opgesteld en gevalideerd met waardes uit de literatuur. De chemische evolutie van cement bij blootstelling aan opeenvolgende volumes water is gesimuleerd met behulp van de chemische speciatiesoftware PHREEQC en de cement thermodynamische database CEMDATA07. Tijdschalen van uitloging zijn gesimuleerd door diffusief transport en terugkoppeling van chemische veranderingen in de cementchemie toe te voegen aan de fysica van uitloging (veranderingen in porositeit als gevolg van oplossing en precipitatie van cementmineralen).

Het diffusief-transportmodel was in staat de neerslag van calciet te simuleren, wat resulteerde in een beschermende deklaag calciet op de binnenlagen van de gesimuleerde cementleiding. De calcietlaag verminderde de porositeit van de cellen grenzend aan de drinkwatergrens, waardoor de diffusie werd beperkt, hetgeen resulteerde in minder uitloging. Dit gedrag wordt echter niet voorspeld door de SI van calciet alleen. De SI van calciet voorspelde het gedrag van cement alleen wanneer de cementchemie alleen werd gemodelleerd met evenwicht van opeenvolgende volumes water (zonder terugkoppeling van cementchemie naar fysische veranderingen in porositeit). In dit geval gedroeg calciet zich zoals verwacht - een negatieve SI kwam overeen met het oplossen van calciet, terwijl een positieve SI resulteerde in het neerslaan van calciet. De SI voorspelde echter niet het uitlooggedrag in het diffusiemodel, waarbij veranderingen in de cementchemie samenhingen met veranderingen in de cementporositeit. Terugkoppeling van cementchemie op cementmicrostructuur resulteerde in een complexer verband tussen de watersamenstelling en het uitlooggedrag, dat niet in de eenvoudige SI werd vastgelegd.

Dit betekent dat het volgens ons model niet mogelijk is het uitlooggedrag van cementbuizen te voorspellen op basis van de SI van calciet voor het instromende water. Mogelijk is een combinatie van indexparameters of een grondiger eanalyse van de watersamenstelling nodig om zinvol inzicht te verschaffen in het uitlooggedrag bij verschillende watersamenstellingen. In een vervolgproject zal de relatie tussen watersamenstelling, indexparameters en het uitlooggedrag van cement systematisch moeten worden onderzocht.

5.2 Gevolgen voor de drinkwaterbedrijven

Ingediend door de waterbedrijven: Wat zijn de gevolgen hiervan in de praktijk voor de drinkwaterbedrijven?

PWN wenst een tool om naast destructief onderzoek, zogenaamde “lakmoesproef”, op basis van modelberekeningen de verwachte conditie van asbestcementleidingen te bepalen. Uit dit initiële onderzoek blijkt dat het model de bekende gegevens uit de praktijk nog niet voldoende goed beschrijft.

Oasen constateert dat het lastig is om bij het gebruik van RO te voldoen aan de wettelijke ondergrens van de SI. Ze willen daarom weten of SI de juiste parameter is om de uitloging van asbest-cement leidingen te beheersen. Dit onderzoek is een mooie stap op weg naar het antwoord. Er zijn in dit project bemoedigende resultaten behaald en de verwacht dat het vervolgonderzoek nog dichter bij het antwoord komt.

Met de uitkomsten kan Oasen dan de keuze maken op welke manier het de uitloging van asbest-cementen leidingen kan voorkomen rekening houdend met verschillende aspecten waaronder duurzaamheid.

Dit onderzoek bevestigt voor WLN dat de SI een rol speelt bij het oplossen van cementhoudende materialen, maar het heeft ook duidelijk gemaakt dat het complexe geheel van oplossen en neerslaan van calciet zeker niet alleen afhangt van de SI, maar van de watersamenstelling als geheel. Verder onderzoek is dan ook nodig om na te gaan of er belangrijkere indexparameters zijn die bovengenoemde processen beter en volledig kunnen beschrijven, met als uiteindelijk doel het ontwikkelen van een tool die bruikbaar is voor de waterbedrijven voor asset management doeleinden.

De conclusie dat niet het mogelijk is het uitlooggedrag van cementbuizen te voorspellen op basis van alleen de SI van calciet is voor Vitens relevant. Voor zover bekend is Nederland uniek met een wettelijk norm voor de SI van calciet. Aanpassing van de SI van het drinkwater is op veel Vitens locaties alleen mogelijk door het doseren van natronloog. Vitens is terughoudend met het doseren van natronloog. Omdat hieraan zijn natronloog zijn veiligheidsrisico's verbonden. Daarnaast vergt de fabricage van natronloog veel energie en draagt bij aan de CO_2-footprint van onze productiebedrijven. Het aanpassen van de pH vereist zorgvuldigheid. Als de SI van calciet te hoog wordt kan het water te kalkafzettend worden wat kan leiden tot klachten van klanten.

5.3 Conclusies

- Een diffusief transportmodel van cementhoudende leidingen kan worden gesimuleerd in PhreeqPython dat in staat is de chemische evolutie en de tijdschaal van uitloging te voorspellen voor verschillende cement- en watersamenstellingen. Het model is gevalideerd met waarden uit de literatuur. Het chemisch-evenwichtsmodel is voldoende geverifieerd, terwijl het tijdsafhankelijke (diffusief) model verder onderzoek vereist.

- Aanzienlijke verschillen in berekende uitlogingsnelheid van simulaties met vier watersamenstellingen in het diffusieve transportmodel, ondanks de ogenschijnlijk ongevoeligheid van het model voor veranderingen in de watersamenstelling wanneer alleen cement chemisch evenwicht in aanmerking werd genomen

- Het SI van calciet alleen lijkt onvoldoende om het gedrag en de tijdschaal van uitloging voor verschillende watersamenstellingen te karakteriseren. Het model toont een complexe relatie tussen het uitlooggedrag van cement en de watersamenstelling. Meer onderzoek is nodig om een betere indexparameters of combinatie van parameters te vinden om uitloging te karakteriseren.

- Neerslag van calciet werd door het model gesimuleerd, maar er is meer onderzoek nodig om de effecten van calcietneerslag op veranderingen in porositeit, en daarmee het uitlooggedrag van het cement, beter te kunnen beschrijven.

5.4 Aanbevelingen

Verbetering van het model

- Een systematische evaluatie van de hypothesen die aan het diffusiesmodel ten grondslag liggen. Met name aandacht voor het specifieke asbestcement dat het meest is gebruikt in de distributienetwerken (productieomstandigheden, minerale samenstelling, porositeit, enz.), de invloed van het distributiesysteem (hydraulische omstandigheden, debieten) en de aanname van een representatieve diffusiecoëfficiënt voor alle chemische elementen.

- Verdere validering van het model, met de nadruk op validering vanuit de praktijk. Er worden twee casestudies aanbevolen die een waardevol inzicht kunnen geven in de prestaties van het model bij praktijkomstandigheden. Casestudies dienen in overleg met de projectgroep gekozen te worden voor locaties waar de (historische) watersamenstelling bekend is en waar ook de condities van de leidingen

regelmatig zijn gemonitord. Een mogelijkheid is de transportleiding bij PWN (Heemskerk) die industriewater met een constante samenstelling transporteert en die regelmatig wordt getest op uitloging

- Een gevoeligheidsanalyse van de invloed van variatie in drinkwatersamenstelling op uitlogingspercentages en ontwikkeling van beschermingslagen en een interpretatie van de drinkwatersamenstellingen die het beste blijken te beschermen tegen uitloging van cementhoudende materialen

Toepassing van het model bij drinkwaterbedrijven

- Een systematisch overzicht van de mate waarin de verschillende indexparameters die zijn afgeleid van de drinkwatersamenstelling (ten minste SI, pH en CCPP) de uitlogingspercentages kunnen karakteriseren. In combinatie met de gevoeligheidsanalyse moeten de resultaten van de beoordeling worden vertaald in aanbevelingen voor de ontwikkeling (een combinatie van) indexparameters die geschikt zijn om te fungeren als indicatoren van drinkwaterparameters die kunnen worden beherst om uitloging in cementhoudende materialen te voorkomen.

- Opschaling van het model om het te gebruiken voor assetmanagementdoeleinden. Gebruik van het model om de uitlogingsnelheden te voorspellen met de input van water- en cementsamenstelling.

6 References

Appelo, C. A. J., & Postma, D. (2005). *Geochemistry, groundwater and pollution* (2nd Editio). A.A. Balkema Publishers.

Bejaoui, S., & Bary, B. (2007). Modeling of the link between microstructure and effective diffusivity of cement pastes using a simplified composite model. *Cement and Concrete Research*, *37*(3), 469–480. https://doi.org/10.1016/j.cemconres.2006.06.004

Bentur, A., Mindess, S., & Banthia, N. (1999). The Interfacial Transition Zone in Fiber Reinforced Cement and Concrete State-of-the-Art Report of RILEM Eds. In M. . Alexander, G. Arliguie, G. Ballivy, A. Bentur, & J. Marland (Eds.), *Engineering and Transport Properties of the Interfacial Transition Zone in Cementitious Composites*. Retrieved from https://www.rilem.net/publication/publication/84?id_papier=87

Brouwers, H. J. H. (2004). The work of Powers and Brownyard revisited: Part 1. *Cement and Concrete Research*, *34*(9), 1697–1716. https://doi.org/10.1016/j.cemconres.2004.05.031

Carde, C., & François, R. (1999). Modelling the loss of strength and porosity increase due to the leaching of cement pastes. *Cement and Concrete Composites*, *21*(3), 181–188. https://doi.org/10.1016/S0958-9465(98)00046-8

Elzenda, C. H. J., Meyer, P. B., & Stumphuis, J. (1974). Oriënterend onderzoek naar het vóórkomen van asbest in het Nederlandse drinkwater. *H2O*, *7*(19), 406–410.

Eternit. (1980). *Eternit - Asbestcemen Tabellen*. Retrieved from file:///C:/Users/youhe/Downloads/kdoc_o_00042_01.pdf

Garboczi, E. J., & Bentz, D. P. (1992). Computer simulation of the diffusivity of cement-based materials. *Journal of Materials Science*, *27*(8), 2083–2092. https://doi.org/10.1007/BF01117921

Hu, J., & Stroeven, P. (2005). Depercolation threshold of porosity in model cement: Approach by morphological evolution during hydration. *Cement and Concrete Composites*, *27*(1), 19–25. https://doi.org/10.1016/j.cemconcomp.2004.02.039

Jacques, D. (2009). *Benchmarking of the Cement Model and Detrimental Chemical Reactions Including Temperature Dependent Parameters : Project Near Surface Disposal of Category A Waste at Dessel NIROND-TR 2009–30 E*. Brussels, Belgium.

Jacques, D., Perko, J., Seetharam, S., Mallants, D., & Govaerts, J. (2013). Modelling long term evolution of cementitious materials used in waste disposal. *The Behaviours of Cementittious Materials in Long Term Storage and Disposal of Radioactive Waste - Results of a Coordinated Research Project*, 1–26.

Jacques, D., Šimůnek, J., Mallants, D., Perko, J., & Seetharam, S. C. (2011). Evaluating changes of transport properties of chemically degrading concrete using a coupled reactive transport model. *1st International Symposium on Cement-Based Materials for Nuclear Wastes*, (October).

Jacques, D., Wang, L., Martens, E., & Mallants, D. (2009). *Time dependence of the geochemical boundary conditions for the cementitious engineered barriers of the Belgian surface disposal facility. Project near surface disposal of category A waste at Dessel NIROND-TR 2008–24 E*. Brussels, Belgium.

Jacques, D., Wang, L., Martens, E., & Mallants, D. (2010). Modelling chemical degradation of concrete during leaching with rain and soil water types. *Cement and Concrete Research*, *40*(8), 1306–1313. https://doi.org/10.1016/j.cemconres.2010.02.008

Jacques, D., Wang, L., Martens, E., & Mallants, D. (2011). *Evolution of concrete pore water and solid phase composition during leaching with different types of water Project near surface disposal of category NIROND-TR 2008–24 E V2*. https://doi.org/10.13140/RG.2.1.3860.3764

Lemarchand, E. (2009). Micromechanics Contribution to the Analysis of Diffusion Properties Evolution in Cement-Based Materials Undergoing Carbonation Processes. *Journées Scientifiques Du Groupement MoMaS CIRM*. Retrieved from https://slideplayer.com/slide/4508532/

Lothenbach, B., Matschei, T., Möschner, G., & Glasser, F. P. (2008). Thermodynamic modelling of the effect of temperature on the hydration and porosity of Portland cement. *Cement and Concrete Research*, *38*(1), 1–18. https://doi.org/10.1016/j.cemconres.2007.08.017

Lothenbach, B., & Winnefeld, F. (2006). Thermodynamic modelling of the hydration of Portland cement. *Cement and Concrete Research*, *36*(2), 209–226. https://doi.org/10.1016/j.cemconres.2005.03.001

Mainguy, M., Tognazzi, C., Torrenti, J. M., & Adenot, F. (2000). Modelling of leaching in pure cement paste and mortar. *Cement and Concrete Research*, *30*(1), 83–90. https://doi.org/10.1016/S0008-8846(99)00208-2

Matschei, T., Lothenbach, B., & Glasser, F. P. (2007). Thermodynamic properties of Portland cement hydrates in the system CaO-Al2O3-SiO2-CaSO4-CaCO3-H2O. *Cement and Concrete Research*, *37*(10), 1379–1410. https://doi.org/10.1016/j.cemconres.2007.06.002

Moranville, M., Kamali, S., & Guillon, E. (2004). Physicochemical equilibria of cement-based materials in aggressive environments - Experiment and modeling. *Cement and Concrete Research*, *34*(9), 1569–1578. https://doi.org/10.1016/j.cemconres.2004.04.033

Oh, B. H., & Jang, S. Y. (2004). Prediction of diffusivity of concrete based on simple analytic equations. *Cement and Concrete Research*, *34*, 463–480. https://doi.org/10.1016/j.cemconres.2003.08.026

Parkhurst, D. L., & Appelo, C. a. J. (2013). Description of Input and Examples for PHREEQC Version 3 — A Computer Program for Speciation , Batch-Reaction , One-Dimensional Transport , and Inverse Geochemical Calculations. U.S. Geological Survey Techniques and Methods, book 6, chapter A43, 497 p. *U.S. Geological Survey Techniques and Methods, Book 6, Chapter A43*, 6-43A.

Patel, R. A., Perko, J., Jacques, D., De Schutter, G., Ye, G., & Van Bruegel, K. (2018). Effective diffusivity of cement pastes from virtual microstructures: Role of gel porosity and capillary pore percolation. *Construction and Building Materials*, *165*, 833–845. https://doi.org/10.1016/j.conbuildmat.2018.01.010

Powers, T. ., & Brownyard, T. L. (1946). Studies of the Physical Properties of Hardened Portland Cement Paste. *ACI Journal Proceedings*, *43*(9). https://doi.org/10.14359/8745

Pundsack, F. L. (1956). The Properties of Asbestos. II. The Density and Structure of Chrysotile. *Journal of Physical and Chemical*, *60*(3), 361–364. https://doi.org/10.1021/j150537a027

Richardson, J. F., Harker, J. H., & Backhurst, J. R. (2002). CHAPTER 10 - Leaching. In *Chemical Engineering (Fifth Edition) Volume 2: Particle Technology and Separation Processes* (pp. 502–541). https://doi.org/10.1016/C2009-0-25733-3

Sant, G., Bentz, D., & Weiss, J. (2011). Capillary porosity depercolation in cement-based materials: Measurement techniques and factors which influence their interpretation. *Cement and Concrete Research*, *41*(8), 854–864. https://doi.org/10.1016/j.cemconres.2011.04.006

Slaats, P., Meerkerk, M., & Hofman-Caris, C. (2013). *Conditionering: de optimale samenstelling van drinkwater; Kiwa-Mededeling 100 – Update 2013*. Nieuwegein, Netherlands.

van Laarhoven, K., & van Vossen. (2019). *Beoordeling van methodieken voor het voorspellen van toekomstige storingsfrequenties: resultaten van een pilot met AC. BTO 2019.050*. Nieuwegein, Netherlands.

Vitens. (2021). Vitens/phreeqpython: Object-oriented python wrapper for the VIPhreeqc module. Retrieved May 31, 2021, from https://github.com/Vitens/phreeqpython

I Appendix

I.I Model Assumptions

- Iron is neglected as (Jacques et al., 2009) found it led to unnecessarily complicated calculations and its inclusion had no effect on the evolution of pH, element concentrations and solid phase composition.
- Only diffusive transport, advective transport is assumed to be negligible
- Cement pores are saturated with water and therefore no unsaturated transport
- Neglect electro-diffusive phenomena, therefore each aqueous species has same diffusion coefficient
- Negligible degradation of the cement pipe occurs from the outer pipe and the pipe is sufficiently long to have no boundary effects
- Cement is fully hydrated (α=1), therefore all cement clinker is hydrated leaving no unreacted cement
- Asbestos fibres are chrysotile asbestos, with a density of 2.53 g/cm^3
- Deposition of calcite results in decreased porosity (solid precipitate). Porosity change is calculated based on the molar volume of calcite

I.II Model Equations

The volume of the hydrated cement (V_{hc}) is the sum of hydrated cement minerals;

$$V_{hc} = \sum V_{cement_{minerals}} \qquad \textit{Eq. 11}$$

The gel porosity ($\emptyset_g$) is a function of the volume of CSH-gel.

$$\varphi_g = \frac{V_{gel\ pores}}{V_{hp}} \qquad \textit{Eq. 12}$$

From practice in the literature, the volume fraction of the gel pores (φ_g) is known to be 27-32% of the volume of the hydration product (V_{hp}). Further, the volume fraction of CSH minerals in the hydration product (φ_{CSH}) is known to range between 0.33-0.38 (Brouwers, 2004) and can be calculated as;

$$\frac{V_{CSH}}{V_{hp}} = \varphi_{CSH} \qquad \textit{Eq. 13}$$

The φ_{CSH} can be calculated from the equations above, knowing V_{hc}, V_{CSH} and setting $\varphi_g = 0.27 - 0.32$.

$$\varphi_{CSH} = (1 - \varphi_g) * \frac{V_{CSH}}{V_{hc}} \quad \textit{Eq. 14}$$

Finally γ_{CSH} gives the volume fraction of CSH in the hydration product to the volume fraction of gel pores in the hydration product;

$$\gamma_{CSH} = \frac{\varphi_g}{\varphi_{CSH}} \quad \textit{Eq. 15}$$

Using γ_{CSH} we can calculate the the volume of gel pores directly from the volume of CSH mineral;

$$V_g = \gamma_{CSH} * V_{CSH} \quad \textit{Eq. 16}$$

From the Powers model and data from practice, we also known that the total, gel and capillary porosity can be calculated from the water to cement ratio (wc) and the degree of hydration of the cement (α) (Patel et al., 2018);

$$ø_{total} = \frac{wc - 0.17\alpha}{wc + 0.32} = ø_{cp} + ø_g \quad \textit{Eq. 17}$$

$$ø_{cp} = \frac{wc - 0.36\alpha}{wc + 0.32} \quad \textit{Eq. 18}$$

I.III Chemical model verification

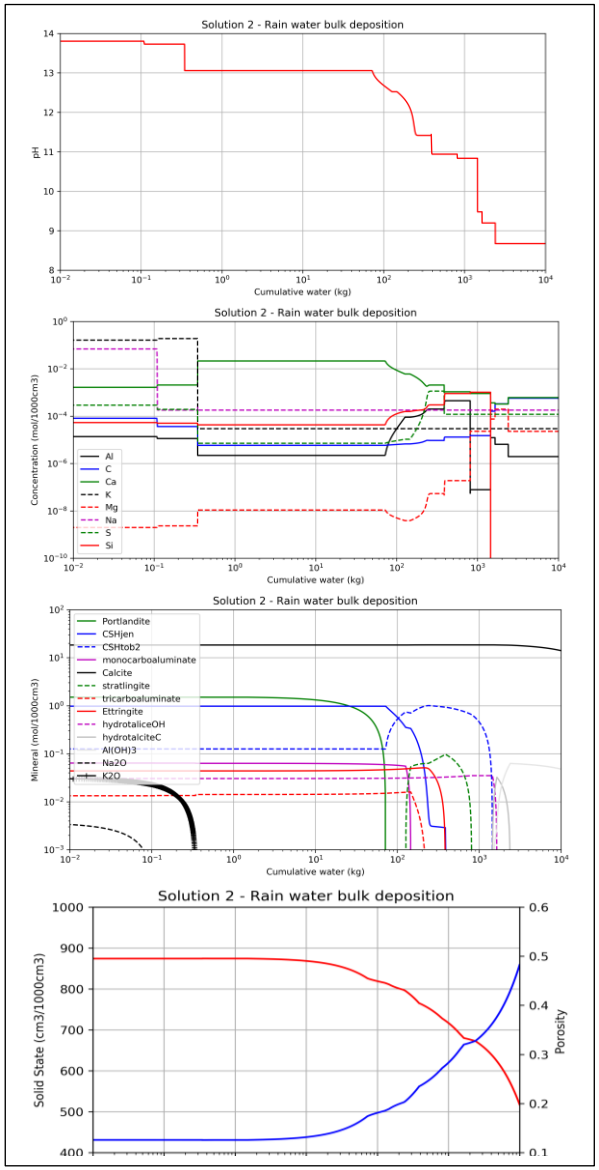

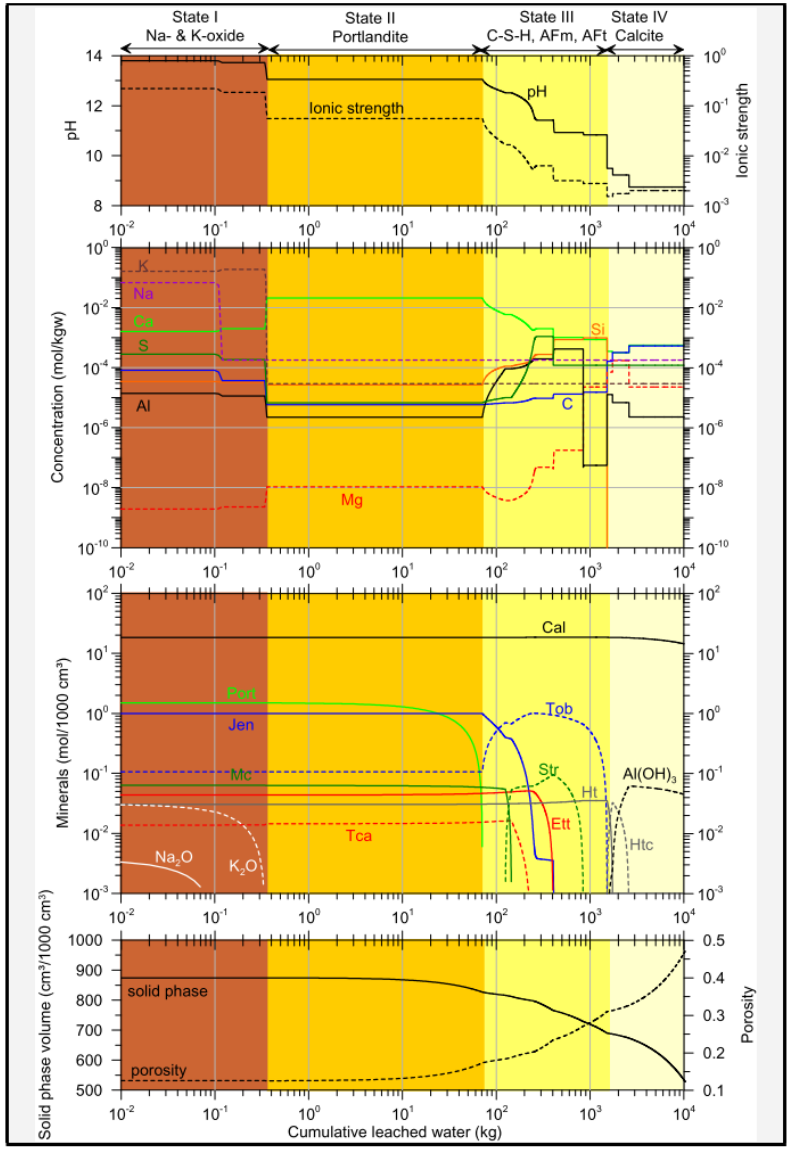

Figure 19 Left, results of the chemical model of leaching of 1000 cm³ of OPC with rain water bulk deposition (water composition 2) at 10°C. Results verified against the model of Jacques et al. (2013), right.

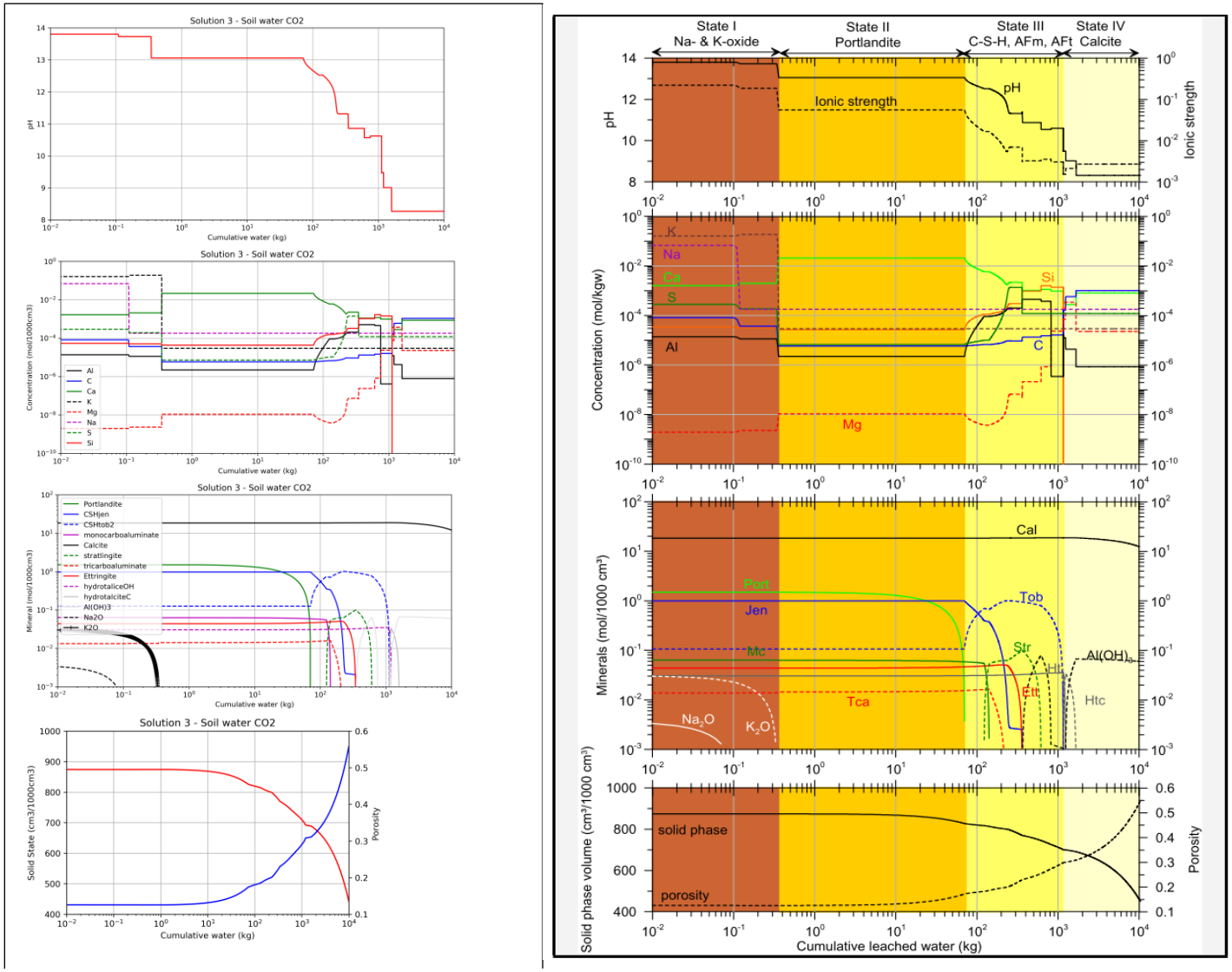

Figure 20 Left, results of the chemical model of leaching of 1000 cm³ of OPC with soil water CO_2 (water composition 3) at 10°C. Results verified against the model of Jacques et al. (2013), right.

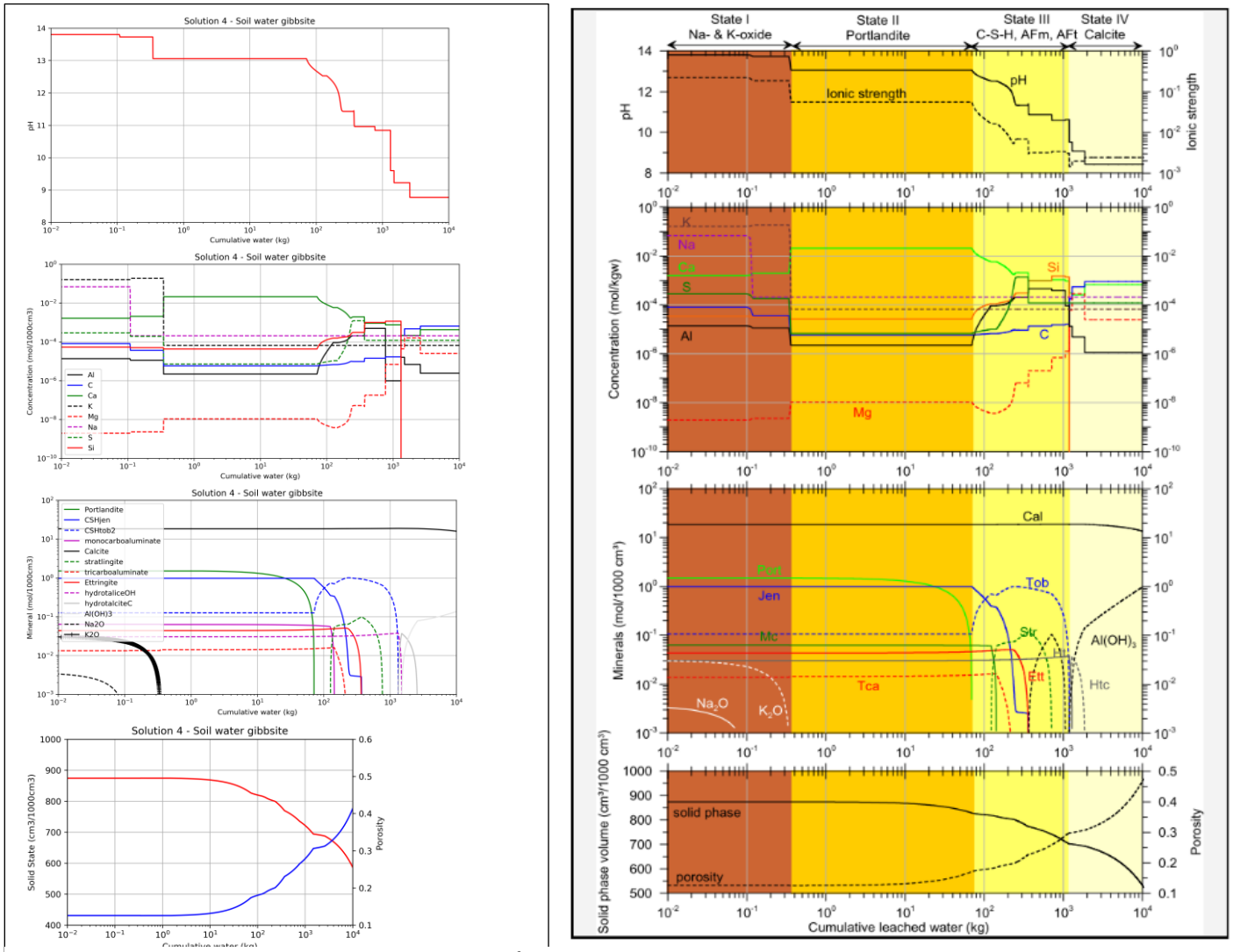

Figure 21 Left, results of the chemical model of leaching of 1000 cm³ of OPC with soil water gibbsite (water composition 4) at 10°C. Results verified against the model of Jacques et al. (2013), right.

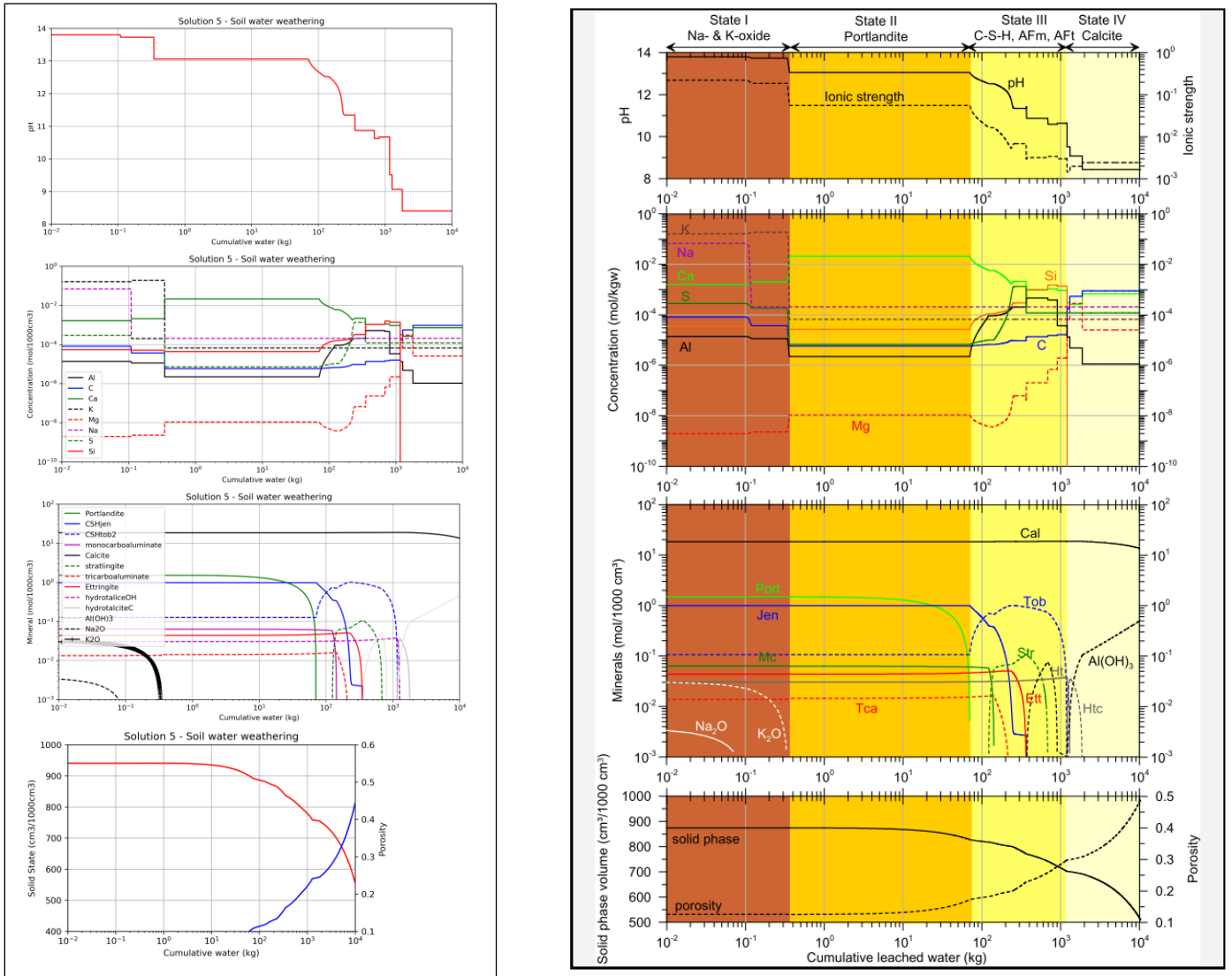

Figure 22 Left, results of the chemical model of leaching of 1000 cm³ of OPC with soil weathering (water composition 5) at 10°C. Results verified against the model of Jacques et al. (2013), right.

I.IV Chemical drinking water simulation results

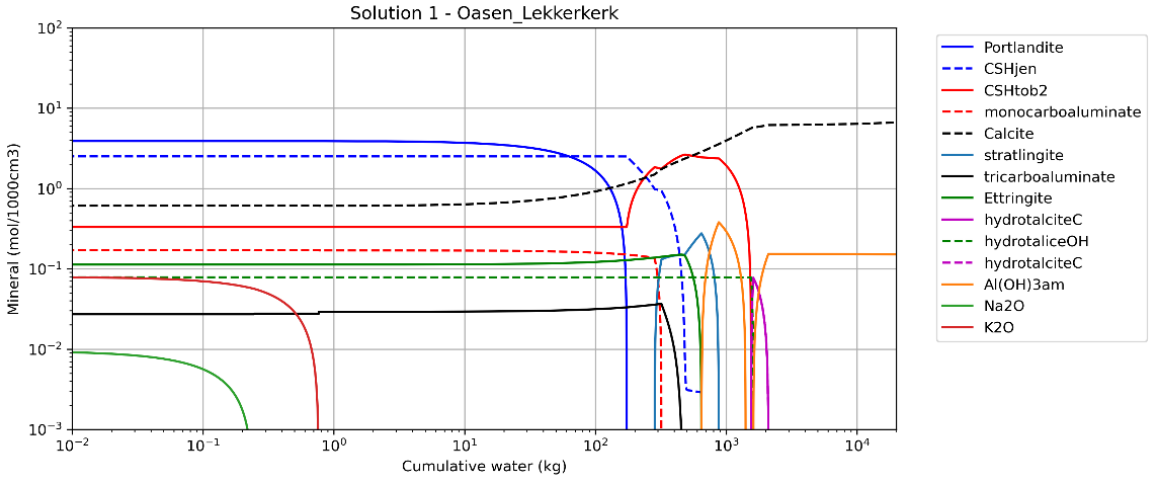

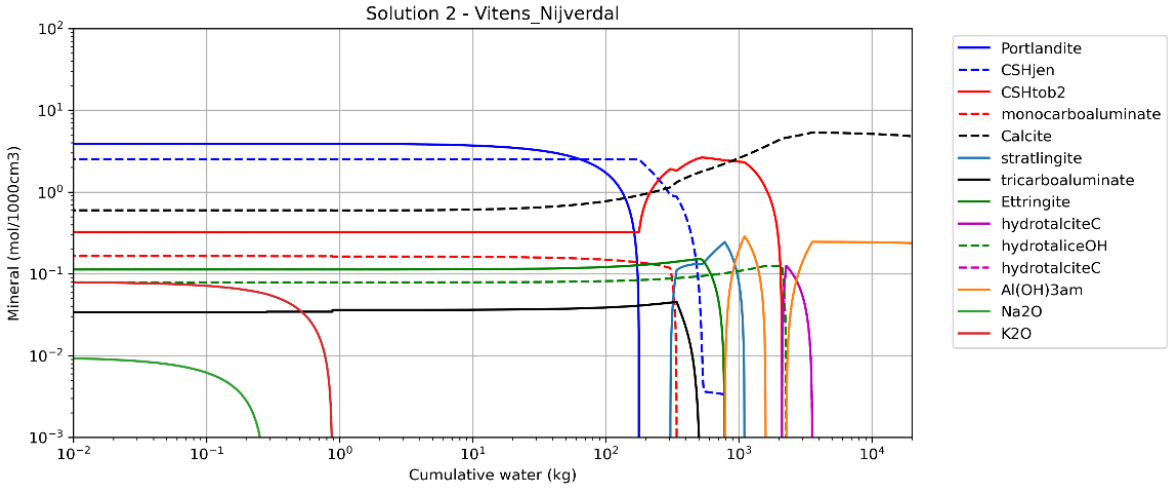

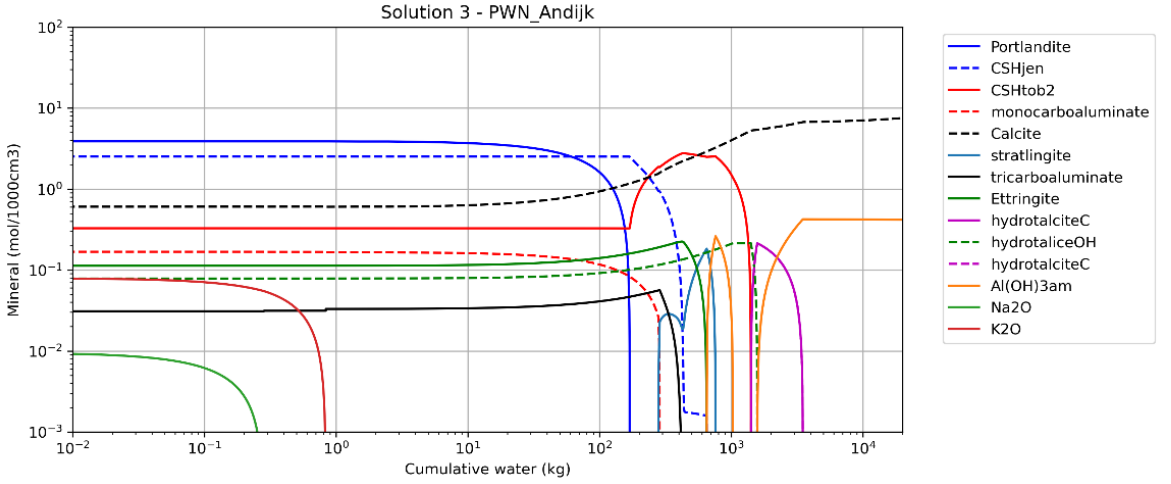

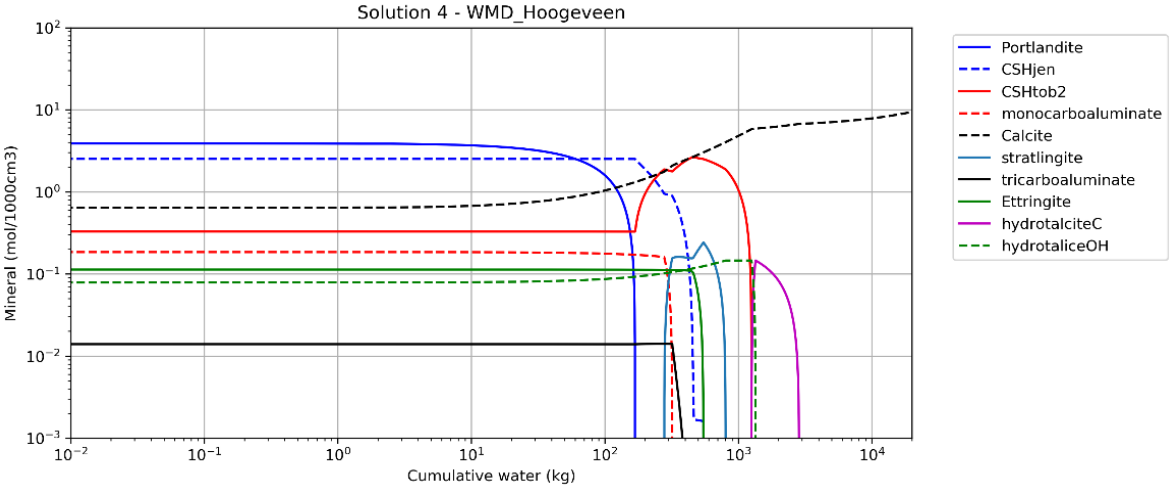
Solution 4 - WMD_Hoogeveen
Mineral (mol/1000cm3)
Cumulative water (kg)
Portlandite
CSHjen
CSHtob2
monocarboaluminate
Calcite
stratlingite
tricarboaluminate
Ettringite
hydrotalciteC
hydrotaliceOH